Climate change impacts on banana yields around the world

Supplementary Information

Varun Varma & Daniel P. Bebber

Supplementary tables

Supplementary table S1. Source, administrative scale and timespan of production data availability for each country used in the analysis. The values in the 'No. obs' column indicates total number of observations for the respective countries that were used in the analysis. Values in brackets indicate the number of geographic units (or administrative units) for which data were available.

Region	Country	Code	Data Source	Data resolution	Timespan	No. obs
Africa	Angola	AO	FAO – http://www.fao.org/faostat/	Country	1969 – 2016	48 (1)
	Burundi	BI	FAO – http://www.fao.org/faostat/	Country	1970 – 2016	47 (1)
	Cameroon	CM	FAO – http://www.fao.org/faostat/	Country	1961 – 2016	56 (1)
	D.R. Congo	CD	FAO – http://www.fao.org/faostat/	Country	1969 – 2016	48 (1)
	Ethiopia	ET	FAO – http://www.fao.org/faostat/	Country	2001 – 2016	56 (1)
	Guinea	GN	FAO – http://www.fao.org/faostat/	Country	1962 – 2016	55 (1)
	Ivory Coast	CI	FAO – http://www.fao.org/faostat/	Country	1961 – 2016	56 (1)
	Kenya	KE	FAO – http://www.fao.org/faostat/	Country	1975 – 2016	42 (1)
	Rwanda	RW	FAO – http://www.fao.org/faostat/	Country	1990 – 2016	27 (1)
	Tanzania	TZ	FAO – http://www.fao.org/faostat/	Country	1992 – 2016	25 (1)
Brazil	Brazil	BR	IBGE – https://sidra.ibge.gov.br/pesquisa/pam/tabelas	Municipality	2001 – 2015	7999 (835)
China	China	CN	National Bureau of Statistics of China - http://data.stats.gov.cn/	Province	1978 – 2015	257 (8)
India	India	IN	Directorate of Economics and Statistics - https://eands.dacnet.nic.in/	District	1997 – 2015	2601 (306)
LAC	Belize	BZ	FAO – http://www.fao.org/faostat/	Country	1989 – 2016	28 (1)
	Colombia	CO	Agronet Colombia - http://www.agronet.gov.co/	Department	1987 – 2016	373 (23)
	Costa Rica	CR	FAO – http://www.fao.org/faostat/	Country	1971 – 2016	46 (1)
	Dominican Republic	DO	FAO – http://www.fao.org/faostat/	Country	1961 – 2015	55 (1)
	Ecuador	EC	FAO – http://www.fao.org/faostat/	Country	1961 – 2016	56 (1)
	Guatemala	GT	FAO – http://www.fao.org/faostat/	Country	1961 – 2016	56 (1)
	Honduras	HN	FAO – http://www.fao.org/faostat/	Country	1961 – 2016	56 (1)
	Mexico	MX	FAO – http://www.fao.org/faostat/	Country	1961 – 2016	56 (1)
	Nicaragua	NI	FAO – http://www.fao.org/faostat/	Country	1972 – 2016	45 (1)
	Panama	PA	FAO – http://www.fao.org/faostat/	Country	1961 – 2015	55 (1)
SEAA	Australia	AU	FAO – http://www.fao.org/faostat/	Country	1961 – 2016	56 (1)
	Indonesia	ID	Ministry of Agriculture, Rep. Indonesia - https://aplikasi2.pertanian.go.id/bdsp/	Province	1970 – 2016	1270 (34)
	Malaysia	MY	FAO – http://www.fao.org/faostat/	Country	1969 – 2016	48 (1)
	Philippines	PH	CountrySTAT Philippines - http://countrystat.psa.gov.ph/	Province	1990 – 2016	2071 (79)

Supplementary table S2. Parameter estimates for regional and global climate-yield models (beta function). Values in brackets indicate bootstrapped 95% confidence intervals.

Region	Scale	Tmin	Topt	Tmax	Pmin	Popt	Pmax
Africa	41.29 (±0.92)	10.68 (±0.06)	30.39 (±0.06)	34.42 (±0.05)	474.83 (±4.22)	505.14 (±7.06)	3530.17 (±38.01)
Brazil	17.94 (±0.1)	18.16 (±0.05)	20.06 (±0.05)	33.96 (±0.08)	5.54 (±1.44)	1250.15 (±17.19)	7913.48 (±23.18)
China	27.84 (±0.16)	13.49 (±0.14)	22.02 (±0.04)	30.48 (±0.19)	0.28 (±0.23)	2924.61 (±13.53)	6563.1 (±64.7)
India	40.04 (±0.14)	10.36 (±0.05)	27.54 (±0.02)	30.48 (±0.03)	224.55 (±3.82)	327.39 (±7.91)	5326.87 (±16.72)
LAC	35.88 (±0.09)	20 (±0.004)	26.83 (±0.01)	29.38 (±0.02)	85.48 (±9.39)	2645.8 (±6.44)	5306.98 (±22.25)
SEAA	22.03 (±0.07)	19.38 (±0.15)	24.11 (±0.04)	33.23 (±0.1)	91.76 (±13.58)	1647.26 (±21.67)	7814.64 (±29.34)
Global	21.29 (±0.04)	10.01 (±0.01)	26.7 (±0.02)	34.99 (±0.01)	0.2 (±0.26)	1673.24 (±6.29)	7996.87 (±3.53)

Supplementary table S3. Changes in yield (T.ha^{-1}) at country, region and global scales from the hindcast analysis (1961-2016). Values in brackets indicate 95% confidence intervals. Values are mapped in Supplementary figures 12, 15, 18, 21, 24 and 27.

Region	Country	Country code	Country trend	Regional trend	Global trend
Africa	Angola	AO	2.02 (±0.7)	3.12 (±0.52)	1.37 (± 0.33)
	Burundi	BI	3.14 (±0.7)		
	Cameroon	CM	2.17 (±0.9)		
	D.R. Congo	CD	3.54 (±0.73)		
	Ethiopia	ET	4.37 (±0.73)		
	Guinea	GN	3.73 (±1.49)		
	Ivory Coast	CI	3.99 (±1.35)		
	Kenya	KE	1.9 (±2.17)		
	Rwanda	RW	2.5 (±0.6)		
	Tanzania	TZ	3.84 (±0.75)		
Brazil	Brazil	BR	-0.78 (±0.3)	-0.78 (±0.3)	
China	China	CN	0.84 (±0.87)	0.84 (±0.87)	
India	India	IN	1.16 (±0.93)	1.16 (±0.93)	
LAC	Belize	BZ	7.06 (±1.26)	2.93 (±0.94)	
	Colombia	CO	-0.29 (±1.14)		
	Costa Rica	CR	3.9 (±1.65)		
	Dominican Republic	DO	5.7 (±2.5)		
	Ecuador	EC	2.23 (±1.81)		
	Guatemala	GT	5.1 (±1.01)		
	Honduras	HN	4.87 (±1.12)		
	Mexico	MX	3.68 (±0.88)		
	Nicaragua	NI	3.8 (±1.21)		
	Panama	PA	2.36 (±1.8)		
SEAA	Australia	AU	0.94 (±0.49)	-1.69 (±0.38)	
	Indonesia	ID	-1.6 (±0.71)		
	Malaysia	MY	-1.88 (±0.52)		
	Philippines	PH	-1.8 (±0.41)		

Supplementary table S4. Country-scale changes in climate (temperature trend and precipitation trend) and climate-driven relative yield coefficients for temperature (R_t) and precipitation (R_p) between 1961-2016. R_t and R_p were calculated using equations 1 and 2, and their trends are the annual rate of change as a function of the change in temperature and precipitation, respectively. Greater values of the R_t trend (compared to R_p trend) indicate a stronger effect of changing temperatures on banana yields. Numbers in brackets indicate 95% confidence intervals.

Region	Country	Country code	Temperature trend (°C.y^{-1})	Precipitation trend (mm.y^{-1})	R_t trend (y^{-1})	R_p trend (y^{-1})
Africa	Angola	AO	0.017 (±0.004)	-1.075 (±1.487)	0.0012 (±0.0003)	-0.0001 (±0.0008)
	Burundi	BI	0.023 (±0.004)	-0.709 (±1.855)	0.0017 (±0.0003)	0.0002 (±0.0006)
	Cameroon	CM	0.01 (±0.004)	-1.929 (±1.991)	0.0011 (±0.0004)	0.0007 (±0.0007)
	D.R. Congo	CD	0.017 (±0.003)	-1.979 (±1.274)	0.0018 (±0.0004)	0.0007 (±0.0004)
	Ethiopia	ET	0.028 (±0.004)	-0.799 (±1.83)	0.0022 (±0.0003)	0.0004 (±0.0005)
	Guinea	GN	0.018 (±0.004)	-1.555 (±2.587)	0.0022 (±0.0005)	0.0005 (±0.0009)
	Ivory Coast	CI	0.015 (±0.004)	-1.733 (±2.274)	0.0018 (±0.0005)	0.0006 (±0.0008)
	Kenya	KE	0.025 (±0.004)	-1.881 (±2.354)	0.0022 (±0.0004)	-0.001 (±0.0012)
	Rwanda	RW	0.026 (±0.005)	0.212 (±2.308)	0.0014 (±0.0003)	-0.0001 (±0.0008)
	Tanzania	TZ	0.02 (±0.004)	-2.652 (±1.977)	0.0017 (±0.0003)	0.0007 (±0.0006)
Brazil	Brazil	BR	0.017 (±0.004)	0.666 (±1.833)	-0.0006 (±0.0003)	-0.0002 (±0.0001)
China	China	CN	0.013 (±0.005)	1.136 (±2.594)	0.0006 (±0.0002)	0.0001 (±0.0006)
India	India	IN	0.017 (±0.003)	-0.077 (±2.226)	0.0007 (±0.0002)	0 (±0.0004)
LAC	Belize	BZ	0.022 (±0.003)	2.258 (±4.211)	0.0035 (±0.0006)	0.0005 (±0.0004)
	Colombia	CO	0.014 (±0.005)	2.59 (±6.046)	0 (±0.0004)	-0.0003 (±0.0005)
	Costa Rica	CR	0.018 (±0.005)	-6.862 (±5.152)	0.0019 (±0.0006)	0.0005 (±0.0008)
	Dominican Republic	DO	0.017 (±0.004)	3.019 (±4.129)	0.0029 (±0.0008)	0.0007 (±0.0014)
	Ecuador	EC	0.01 (±0.007)	4.452 (±7.124)	0.0017 (±0.0011)	0.0003 (±0.0008)
	Guatemala	GT	0.025 (±0.004)	1.025 (±4.787)	0.0027 (±0.0004)	0.0001 (±0.0004)
	Honduras	HN	0.022 (±0.004)	-0.541 (±4.702)	0.0028 (±0.0005)	0 (±0.0007)
	Mexico	MX	0.02 (±0.003)	1.336 (±2.374)	0.0018 (±0.0003)	0.0003 (±0.0005)
	Nicaragua	NI	0.019 (±0.004)	-4.724 (±5.248)	0.0022 (±0.0005)	0 (±0.0005)
	Panama	PA	0.014 (±0.005)	-1.591 (±5.06)	0.0019 (±0.0007)	-0.0006 (±0.0006)
SEAA	Australia	AU	0.015 (±0.005)	0.117 (±2.479)	0.0009 (±0.0003)	-0.0001 (±0.0004)
	Indonesia	ID	0.018 (±0.003)	3.577 (±6.291)	-0.0011 (±0.0002)	-0.0003 (±0.0006)
	Malaysia	MY	0.02 (±0.003)	4.38 (±4.451)	-0.0011 (±0.0002)	-0.0005 (±0.0005)
	Philippines	PH	0.017 (±0.003)	7.403 (±5.001)	-0.001 (±0.0002)	-0.0006 (±0.0004)

Supplementary table S5. Predicted yield ($T.ha^{-1}$) changes (by 2050 under RCP 4.5 relative to modelled yields using long-term average climatic conditions between 1970 and 2000. Predictions are made at the country scale and then aggregated to regional and global values. Numbers in brackets indicate 95% confidence intervals. Values are mapped in Supplementary figures 13, 16, 19, 22, 25 and 28.

Region	Country	Country code	Country trend	Regional trend	Global trend
Africa	Angola	AO	4.98 (±1.61)	4.53 (±1.38)	0.59 (± 1.38)
	Burundi	BI	4.41 (±1.12)		
	Cameroon	CM	3.33 (±1.46)		
	D.R. Congo	CD	5.03 (±1.86)		
	Ethiopia	ET	4.42 (±1.33)		
	Guinea	GN	3.67 (±2.06)		
	Ivory Coast	CI	4.96 (±2.87)		
	Kenya	KE	4.22 (±1.28)		
	Rwanda	RW	3.65 (±0.92)		
	Tanzania	TZ	5.29 (±1.69)		
Brazil	Brazil	BR	-1.46 (±0.21)	-1.46 (±0.21)	
China	China	CN	0.48 (±1.56)	0.48 (±1.56)	
India	India	IN	-3.68 (±1.78)	-3.68 (±1.78)	
LAC	Belize	BZ	1.31 (±2.5)	1.5 (±1.63)	
	Colombia	CO	-3.7 (±1.1)		
	Costa Rica	CR	-1.03 (±2.02)		
	Dominican Republic	DO	0.84 (±1.69)		
	Ecuador	EC	6.2 (±1.89)		
	Guatemala	GT	-0.79 (±1.72)		
	Honduras	HN	2.71 (±1.81)		
	Mexico	MX	0.25 (±1.61)		
	Nicaragua	NI	-1.3 (±2.19)		
	Panama	PA	-2.76 (±2.5)		
SEAA	Australia	AU	0.35 (±0.41)	-1.85 (±0.49)	
	Indonesia	ID	-1.21 (±0.46)		
	Malaysia	MY	-2.41 (±0.46)		
	Philippines	PH	-2.09 (±0.51)		

Supplementary table S6. Predicted yield ($T.ha^{-1}$) changes (by 2050 under RCP 8.5 relative to modelled yields using long-term average climatic conditions between 1970 and 2000. Predictions are made at the country scale and then aggregated to regional and global values. Numbers in brackets indicate 95% confidence intervals. Values are mapped in Supplementary figures 14, 17, 20, 23, 26 and 29.

Region	Country	Country code	Country trend	Regional trend	Global trend
Africa	Angola	AO	6.49 (±1.99)	5.66 (±1.69)	0.19 (± 1.86)
	Burundi	BI	5.55 (±1.4)		
	Cameroon	CM	4.43 (±1.79)		
	D.R. Congo	CD	6.4 (±2.28)		
	Ethiopia	ET	5.51 (±1.65)		
	Guinea	GN	4.34 (±2.58)		
	Ivory Coast	CI	5.57 (±3.37)		
	Kenya	KE	5.44 (±1.62)		
	Rwanda	RW	4.83 (±1.13)		
	Tanzania	TZ	6.28 (±2.06)		
Brazil	Brazil	BR	-1.87 (±0.25)	-1.87 (±0.25)	
China	China	CN	0.01 (±1.69)	0.01 (±1.69)	
India	India	IN	-6.25 (±1.89)	-6.25 (±1.89)	
LAC	Belize	BZ	0.02 (±2.7)	0.73 (±1.78)	
	Colombia	CO	-4.32 (±1.16)		
	Costa Rica	CR	-2.97 (±2.24)		
	Dominican Republic	DO	-0.5 (±1.8)		
	Ecuador	EC	6.27 (±2.18)		
	Guatemala	GT	-2.24 (±1.87)		
	Honduras	HN	1.91 (±1.91)		
	Mexico	MX	-0.87 (±1.72)		
	Nicaragua	NI	-3.06 (±2.35)		
	Panama	PA	-5.9 (±2.85)		
SEAA	Australia	AU	0.08 (±0.44)	-2.5 (±0.54)	
	Indonesia	ID	-1.76 (±0.52)		
	Malaysia	MY	-3.07 (±0.48)		
	Philippines	PH	-2.78 (±0.57)		

Supplementary figures

Note on interpretation of model fit figures (supplementary figures 1-7): For clarity, the following model fit figures visualise a three-dimensional surface in two dimensions. In each of the supplementary figures 1-7, panel (a) is the relationship of yield with temperature, when precipitation is held constant (at the estimated optimum). Similarly, panel (b) represents the relationship of yield with total annual precipitation when temperature is held constant (at the estimated optimum). The amount of scatter in observed yields around the fitted curves in supplementary figures 1-7 is a consequence of (a) viewing the three-dimensional raw data in two dimensions, (b) differences in technological inputs in different regions where data come from, but which share similar climatic conditions, (c) change in technological input over time for the same region, and (d) unaccounted for variability (sources are discussed in the methods section; see appendix I for further detailed discussion on model fitting and sources of variation).

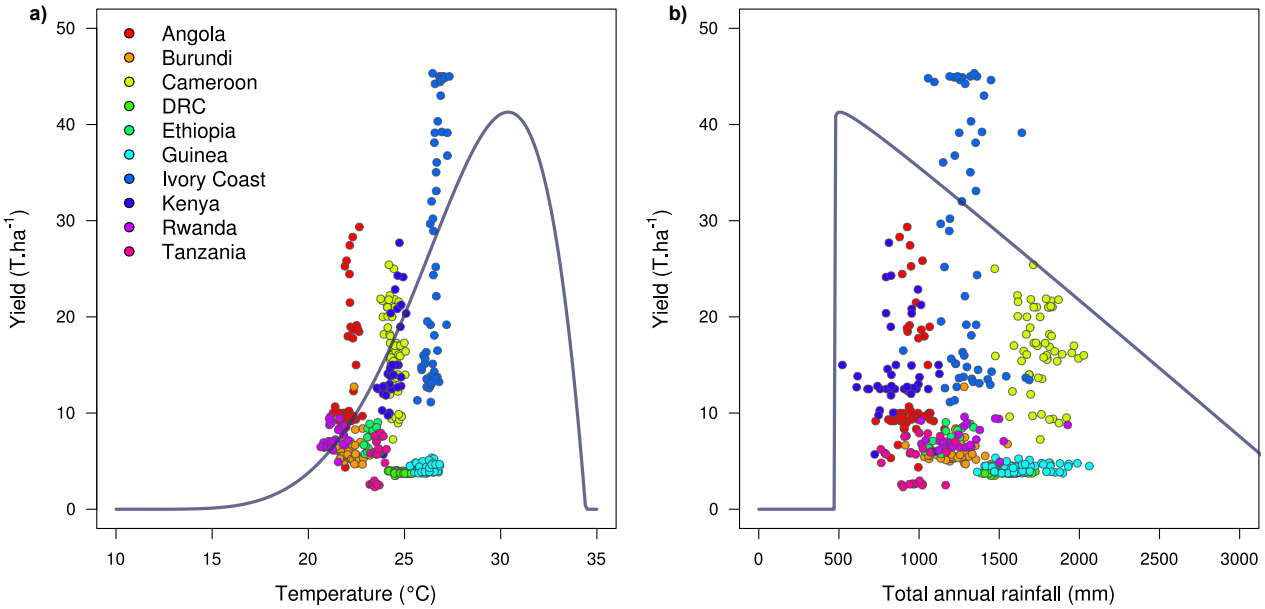

Supplementary figure S1. Observed yield data for Africa and fitted beta functions along the temperature (a) and precipitation (b) axes. The fitted curves represent the best fit beta function (described in equation 3 of the methods), but visualised for temperature and precipitation separately. Parameter estimates for these curves are presented in supplementary table S2.

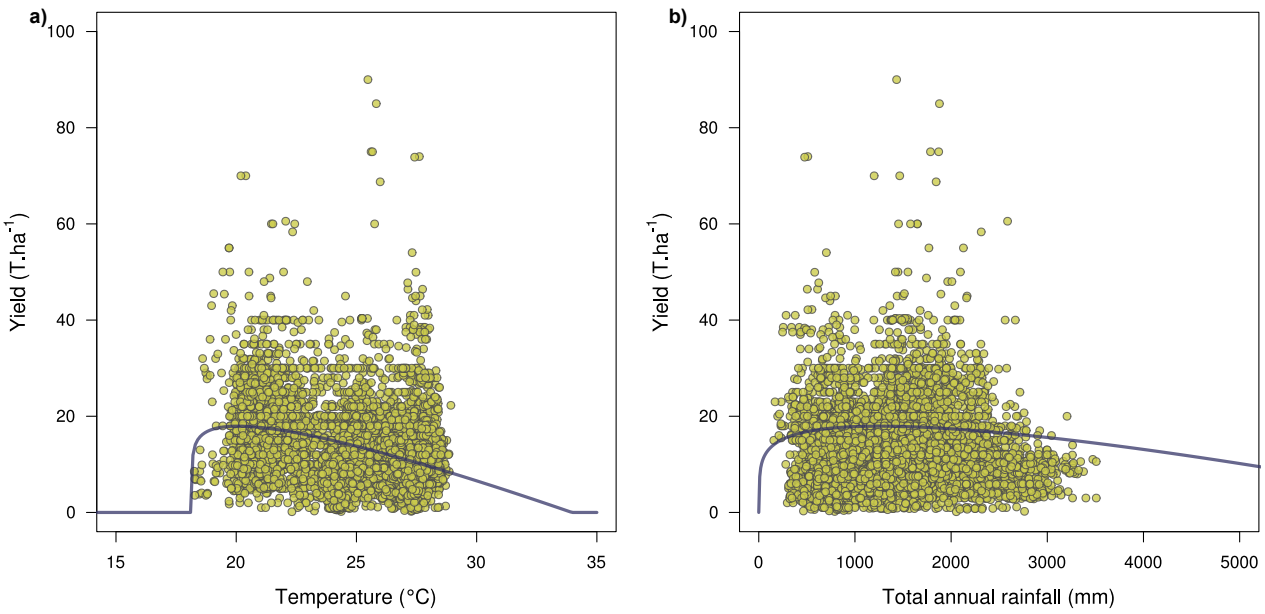

Supplementary figure S2. Observed yield data for Brazil and fitted beta functions along the temperature (a) and precipitation (b) axes. The fitted curves represent the best fit beta function (described in equation 3 of the methods), but visualised for temperature and precipitation separately. Parameter estimates for these curves are presented in supplementary table S2. See Methods for further considerations regarding the Brazil dataset.

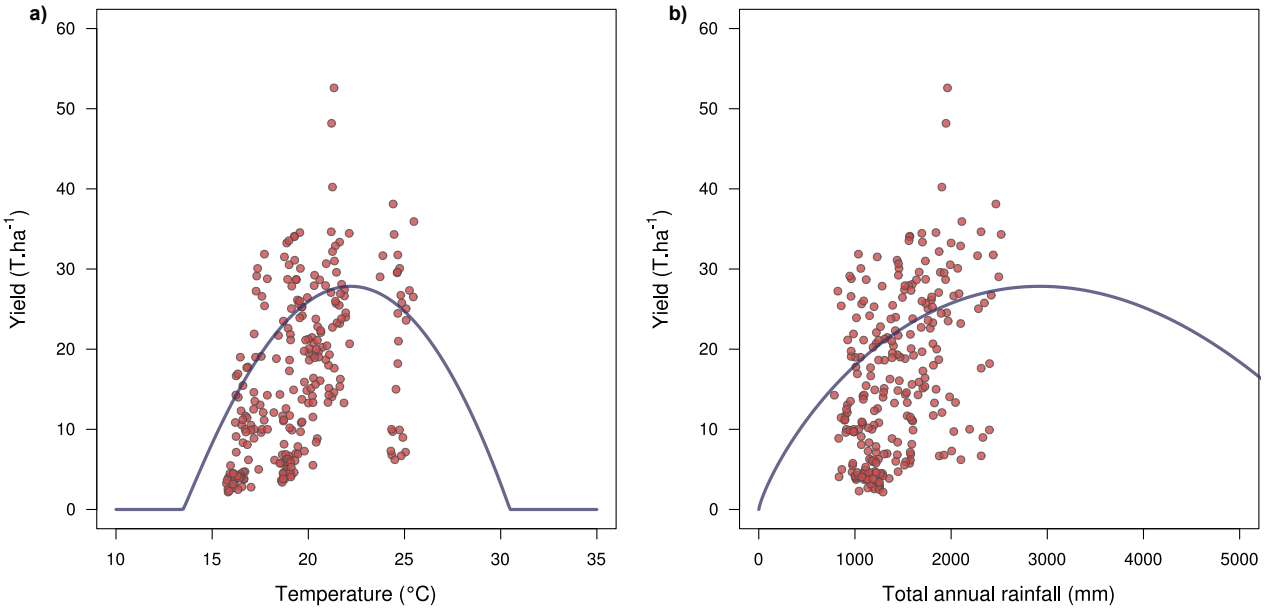

Supplementary figure S3. Observed yield data for China and fitted beta functions along the temperature (a) and precipitation (b) axes. The fitted curves represent the best fit beta function (described in equation 3 of the methods), but visualised for temperature and precipitation separately. Parameter estimates for these curves are presented in supplementary table S2.

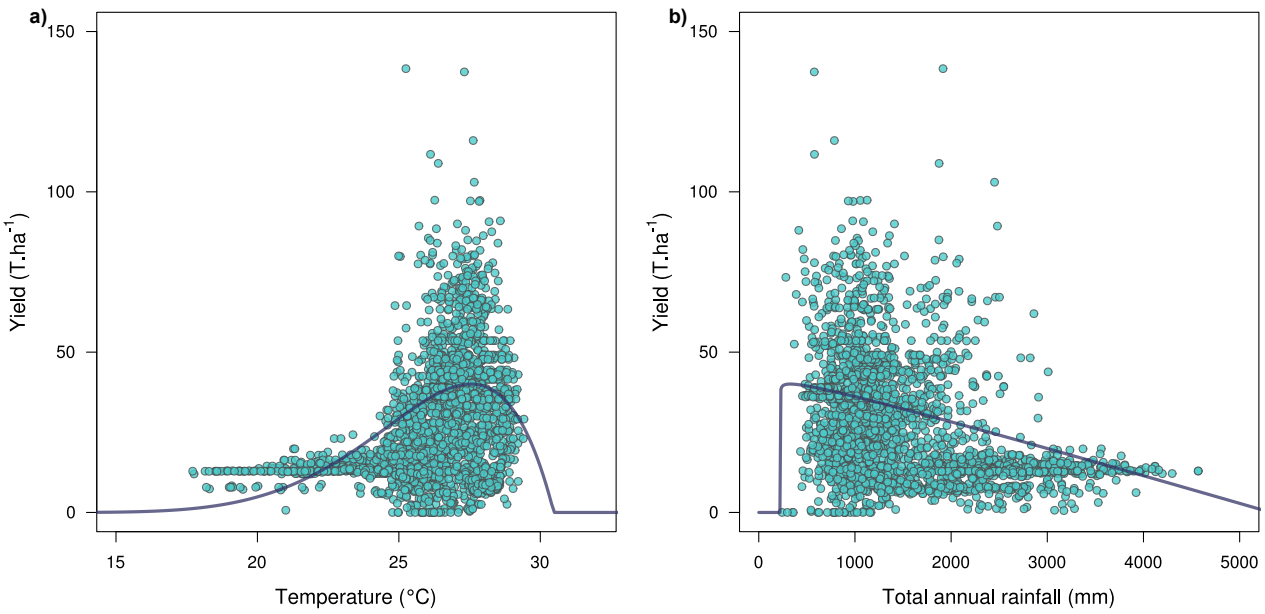

Supplementary figure S4. Observed yield data for India and fitted beta functions along the temperature (a) and precipitation (b) axes. The fitted curves represent the best fit beta function (described in equation 3 of the methods), but visualised for temperature and precipitation separately. Parameter estimates for these curves are presented in supplementary table S2.

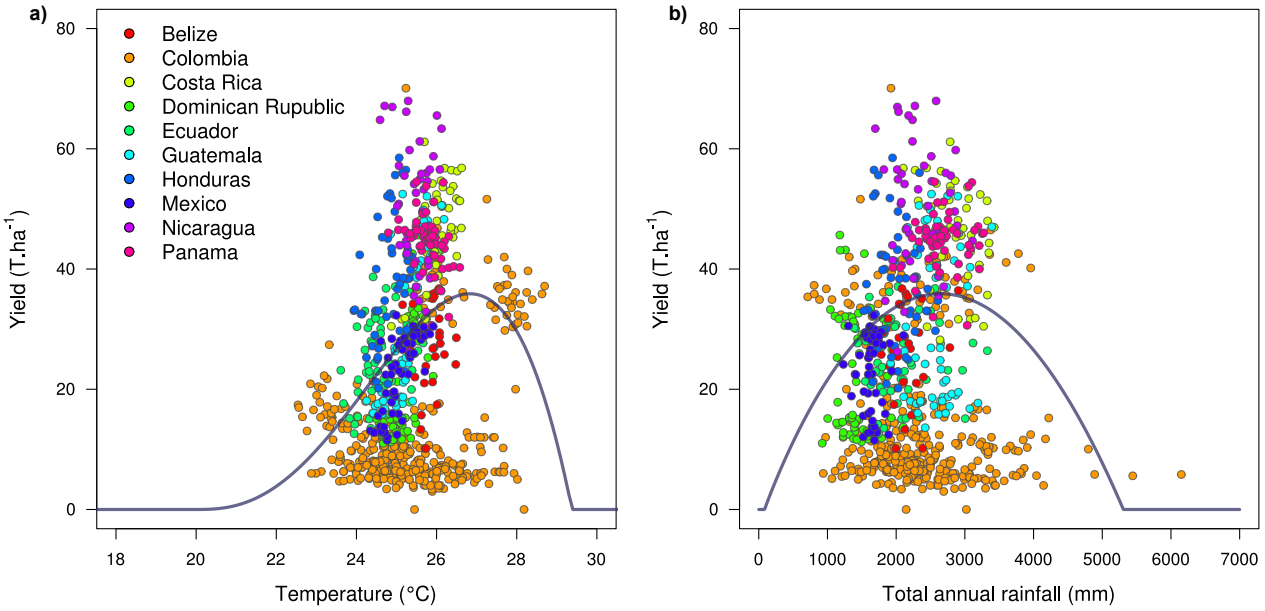

Supplementary figure S5. Observed yield data for Latin America and the Caribbean (LAC) and fitted beta functions along the temperature (a) and precipitation (b) axes. The fitted curves represent the best fit beta function (described in equation 3 of the methods), but visualised for temperature and precipitation separately. Parameter estimates for these curves are presented in supplementary table S2.

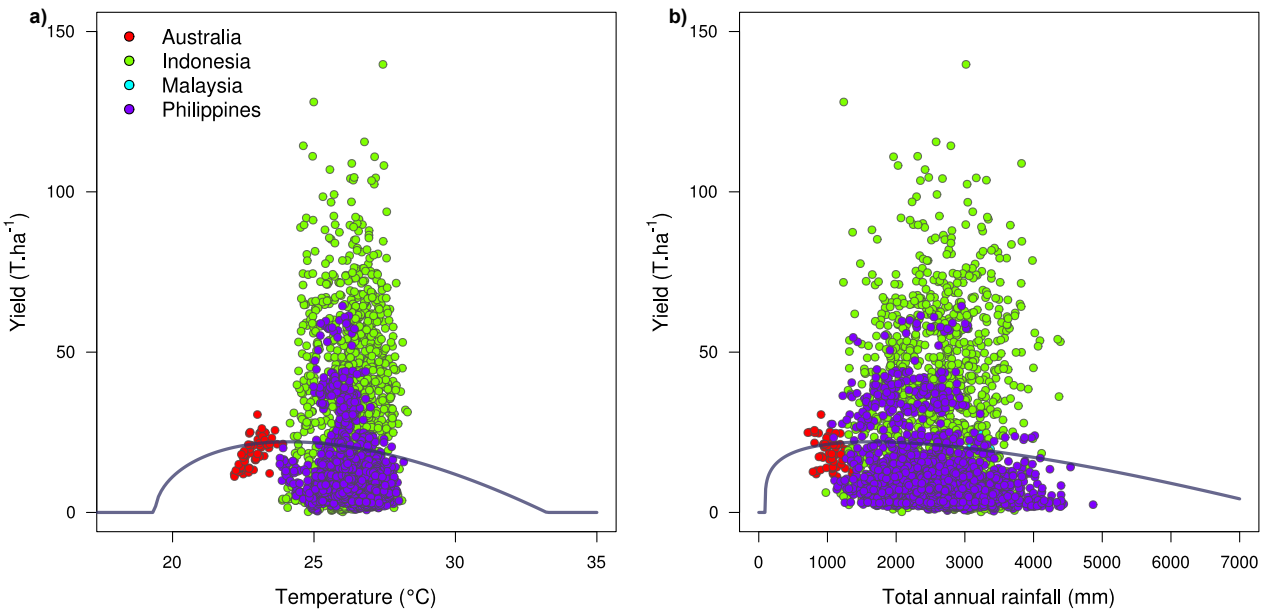

Supplementary figure S6. Observed yield data for South East Asia and Australia (SEAA) and fitted beta functions along the temperature (a) and precipitation (b) axes. The fitted curves represent the best fit beta function (described in equation 3 of the methods), but visualised for temperature and precipitation separately. Parameter estimates for these curves are presented in supplementary table S2.

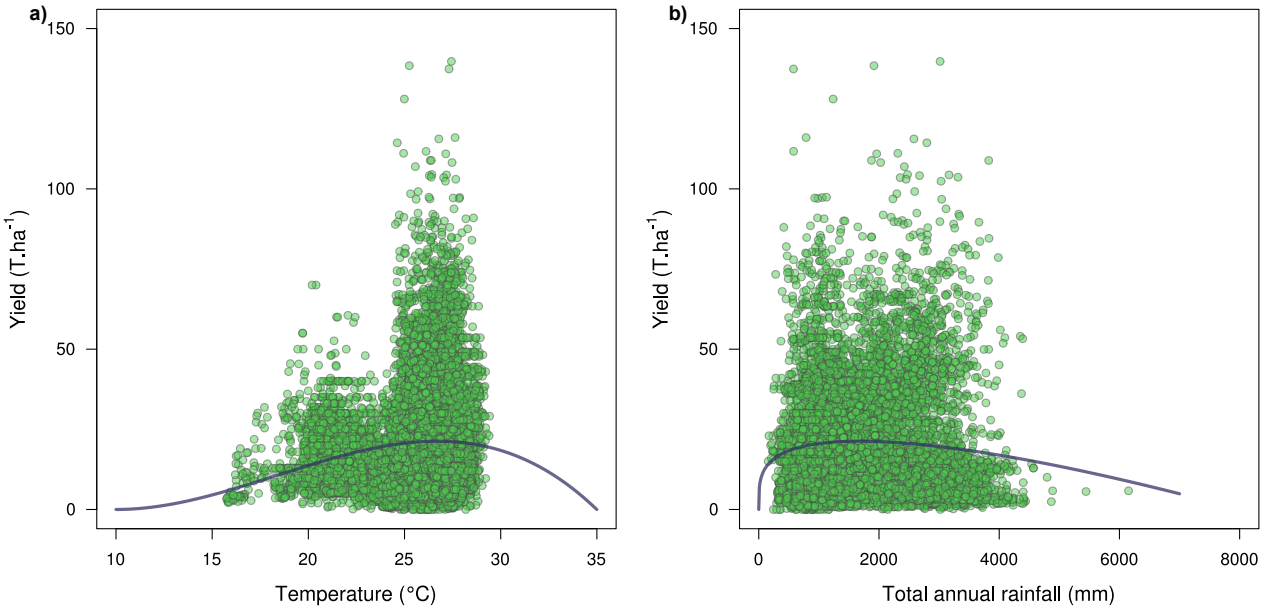

Supplementary figure S7. Observed Global yield data (all countries and regions combined) and fitted beta functions along the temperature (a) and precipitation (b) axes. The fitted curves represent the best fit beta function (described in equation 3 of the methods), but visualised for temperature and precipitation separately. Parameter estimates for these curves are presented in supplementary table S2.

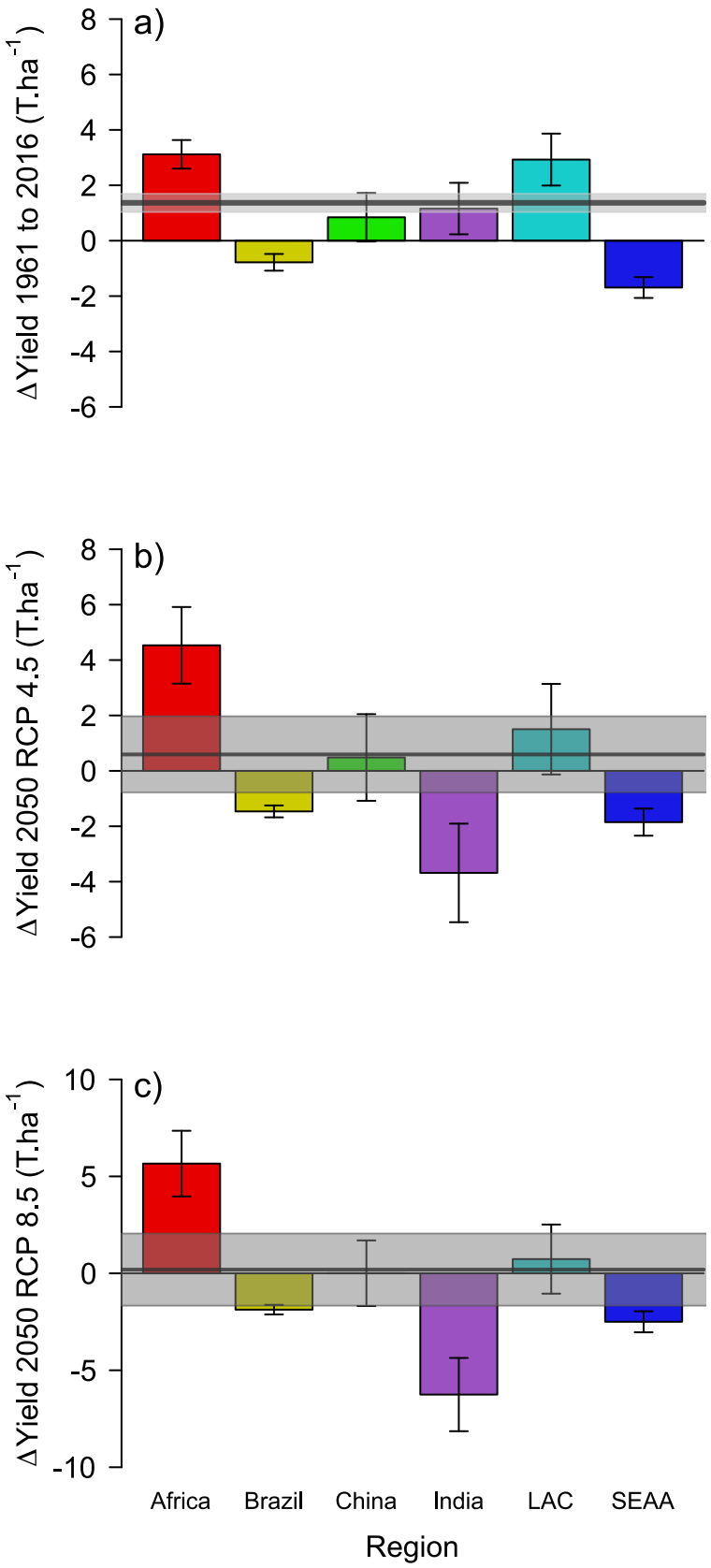

Supplementary figure S8. Regionally averaged yield trend from 1961-2016, i.e. hindcast analysis (a). Regionally averaged change in yields by 2050 under RCP 4.5 (b) and RCP 8.5 (c) relative to yields modelling using long-term climate averages between 1970 and 2000. Black horizontal line and shaded area indicate global averages and associated 95% confidence intervals.

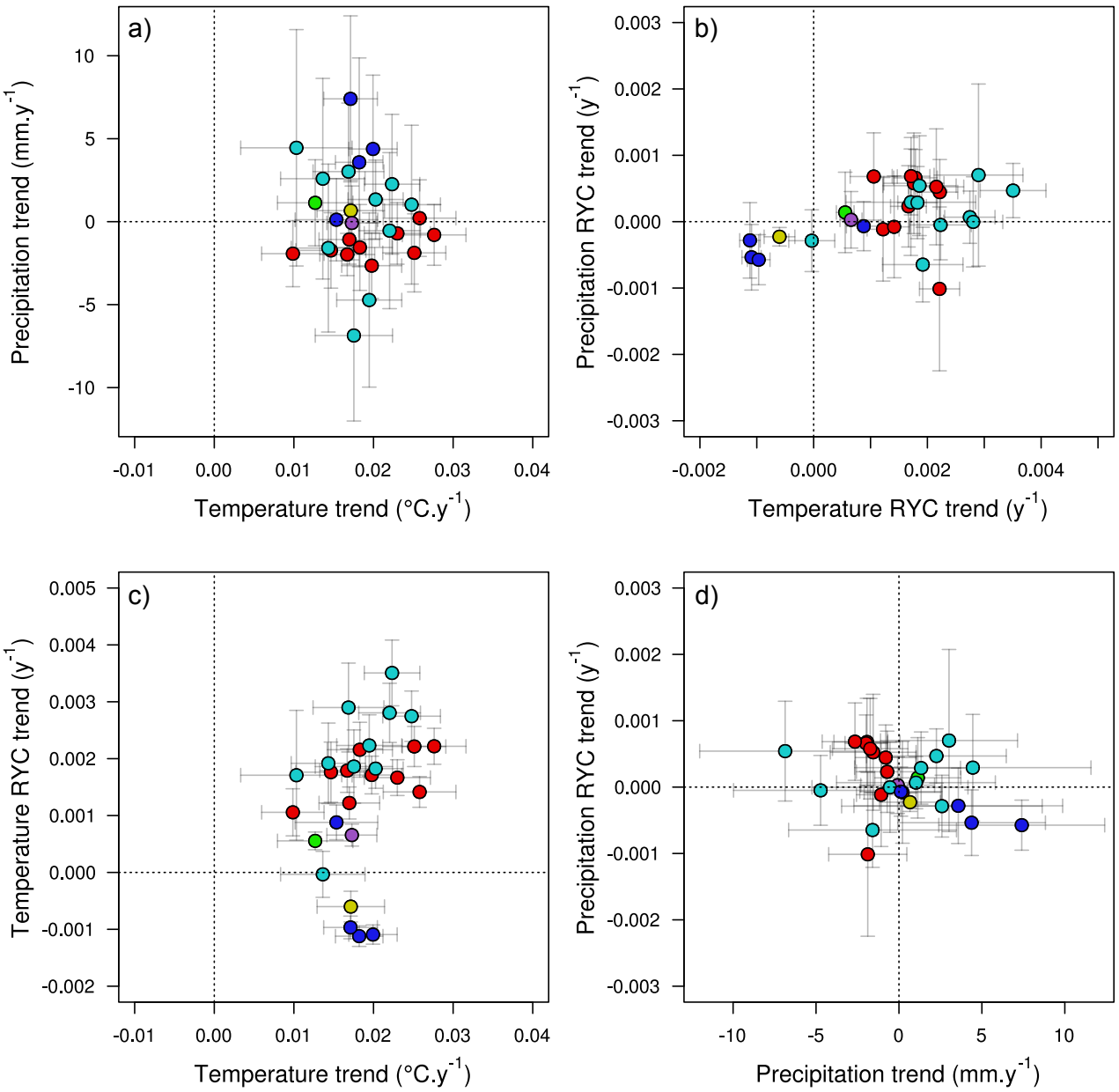

Supplementary figure S9. Isolating the effect of temperature and precipitation on observed yield trends in the past (hindcast analysis; 1961-2016). Biplot of temperature and precipitation trends at a country-scale shows a consistent increase in temperatures for all countries, but a mixed trend for precipitation (a). Biplot of temperature relative yield coefficient (RYC) and precipitation RYC shows a greater spread along the temperature RYC axis (b). Biplot of temperature trend and temperature RYC shows high variation in temperature RYC values for very similar temperature trend values (c), while the opposite is observed in a biplot of precipitation trend and precipitation RYC (d). This suggests that increases in temperature captures far greater variation in observed yields, than changes in precipitation (d). Hence, changes in yield are more likely to be driven by changes in temperature, than changes in precipitation. All countries show an increasing temperature trend, and when this results in temperatures exceeding the optimum for banana cultivation, yield declines are observed. When increasing temperatures approach the optimum, yield gains are likely. No such pattern is observed with precipitation and precipitation RYC. Individual points represent a country, colour coded by region. Error bars represent 95% confidence intervals.

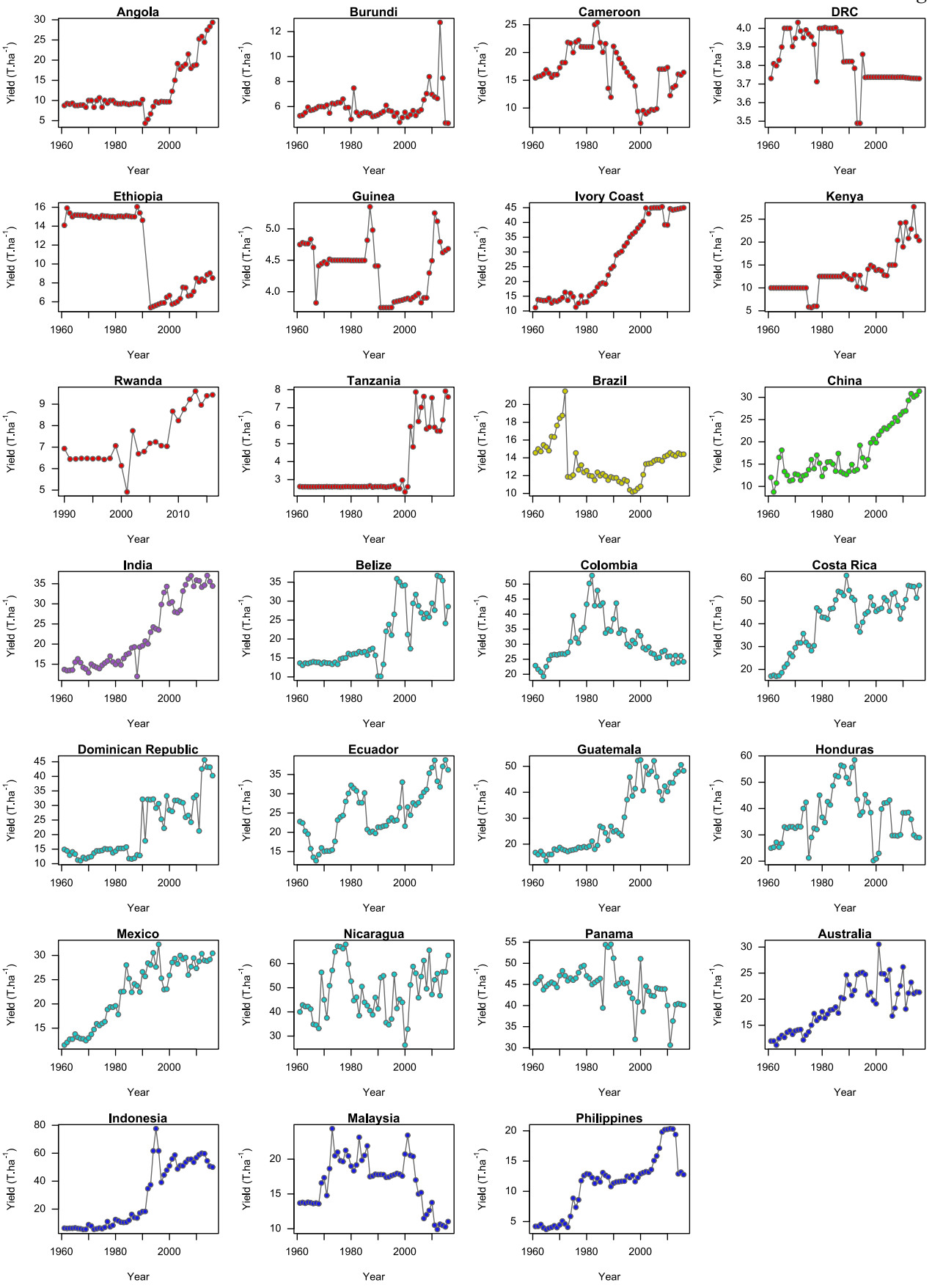

Supplementary figure S10. Production (yield) data for all countries in the analysis over time (data source: FAOSTAT).

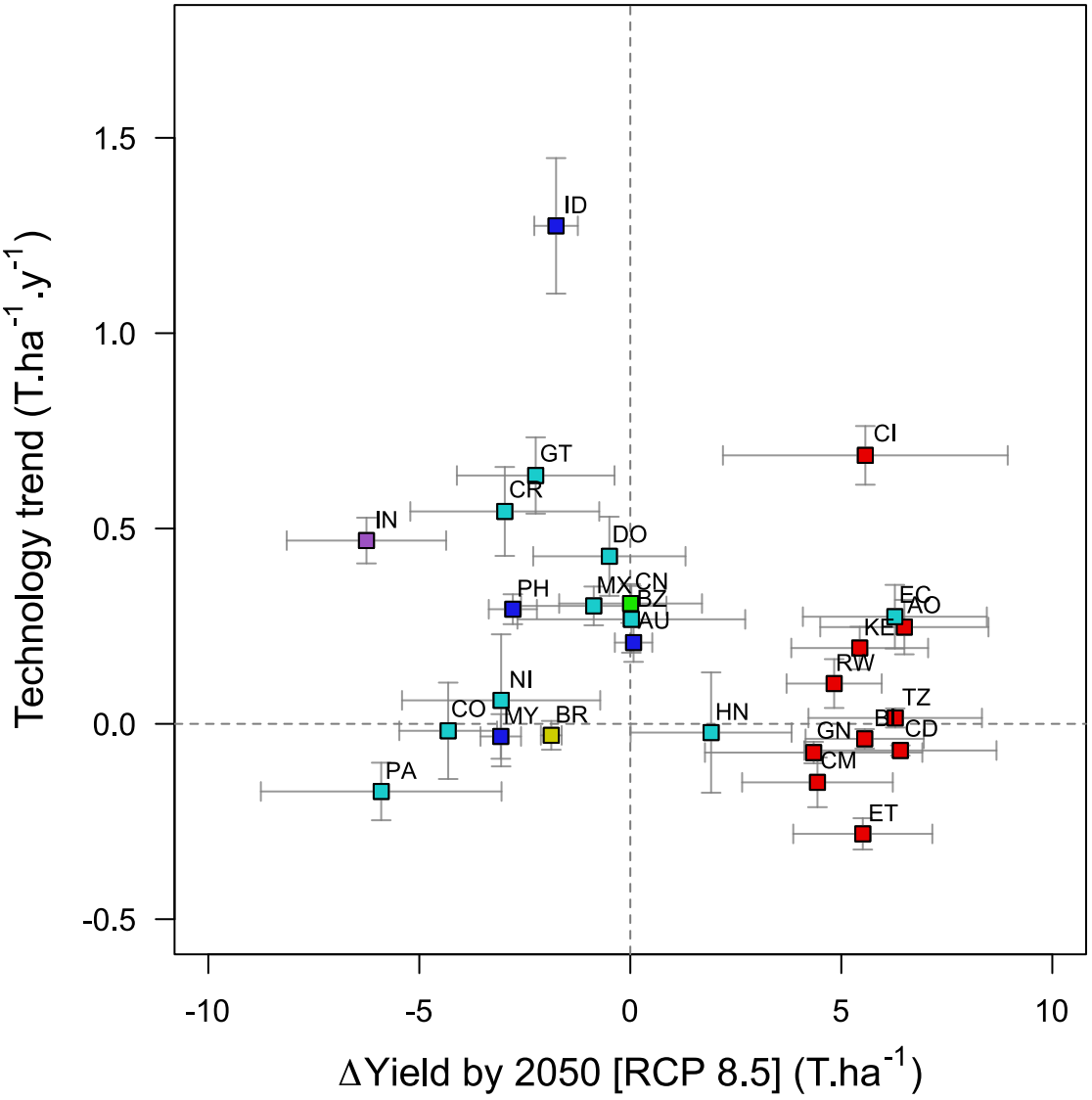

Supplementary figure S11. Classification of future climate risk to major banana producing countries. Countries which fall within the top and bottom right quadrants are predicted to show climate-driven increases in yields by 2050 (RCP 8.5 scenario) and are classified as 'at advantage'. Countries in the top left quadrant could see climate-driven declines in yields, but have strong positive past technology trends, therefore are classified as 'adaptable'. Countries in the lower left quadrant, are predicted to show climate-driven yield declines and also show negative technology trends in the past. These countries are classified as 'at risk'.

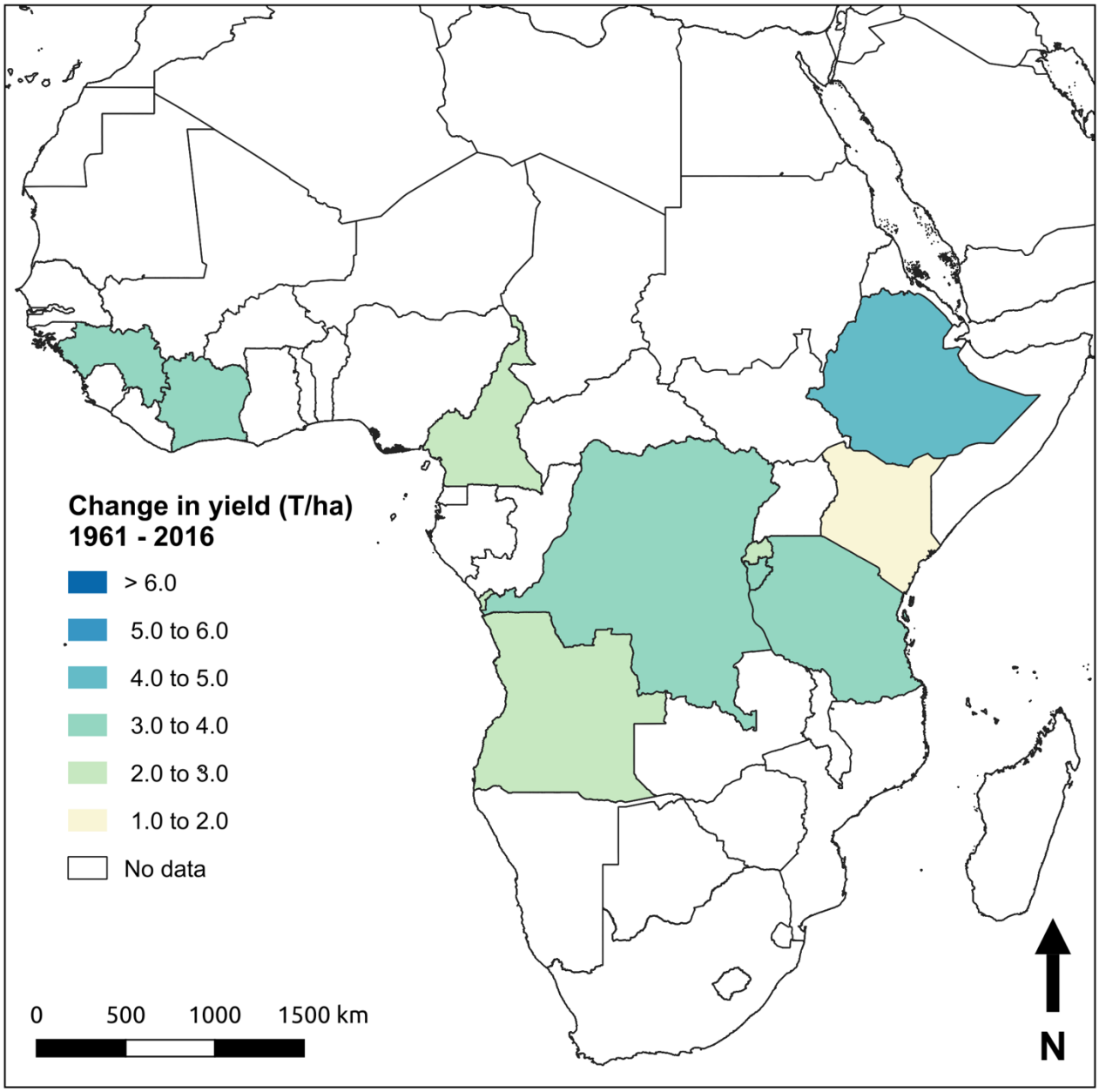

Supplementary figure S12. Map of change in yield for Africa from 1961-2016 estimated using the hindcast analysis.

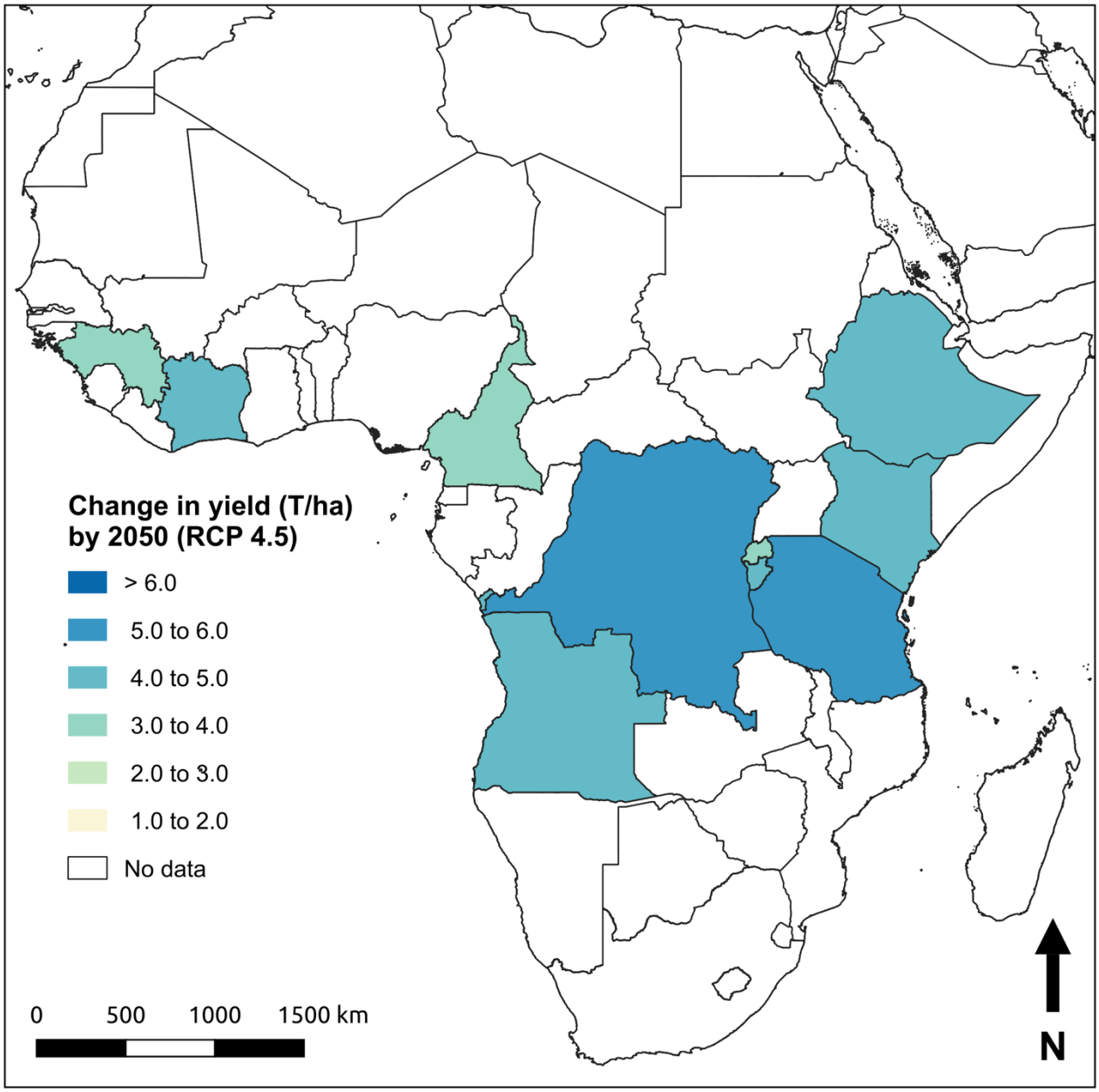

Supplementary figure S13. Map of change in forecasted yields for Africa by 2050 under the RCP 4.5 climate change scenario (relative to yields estimated using long-term climate averages between 1970-2000).

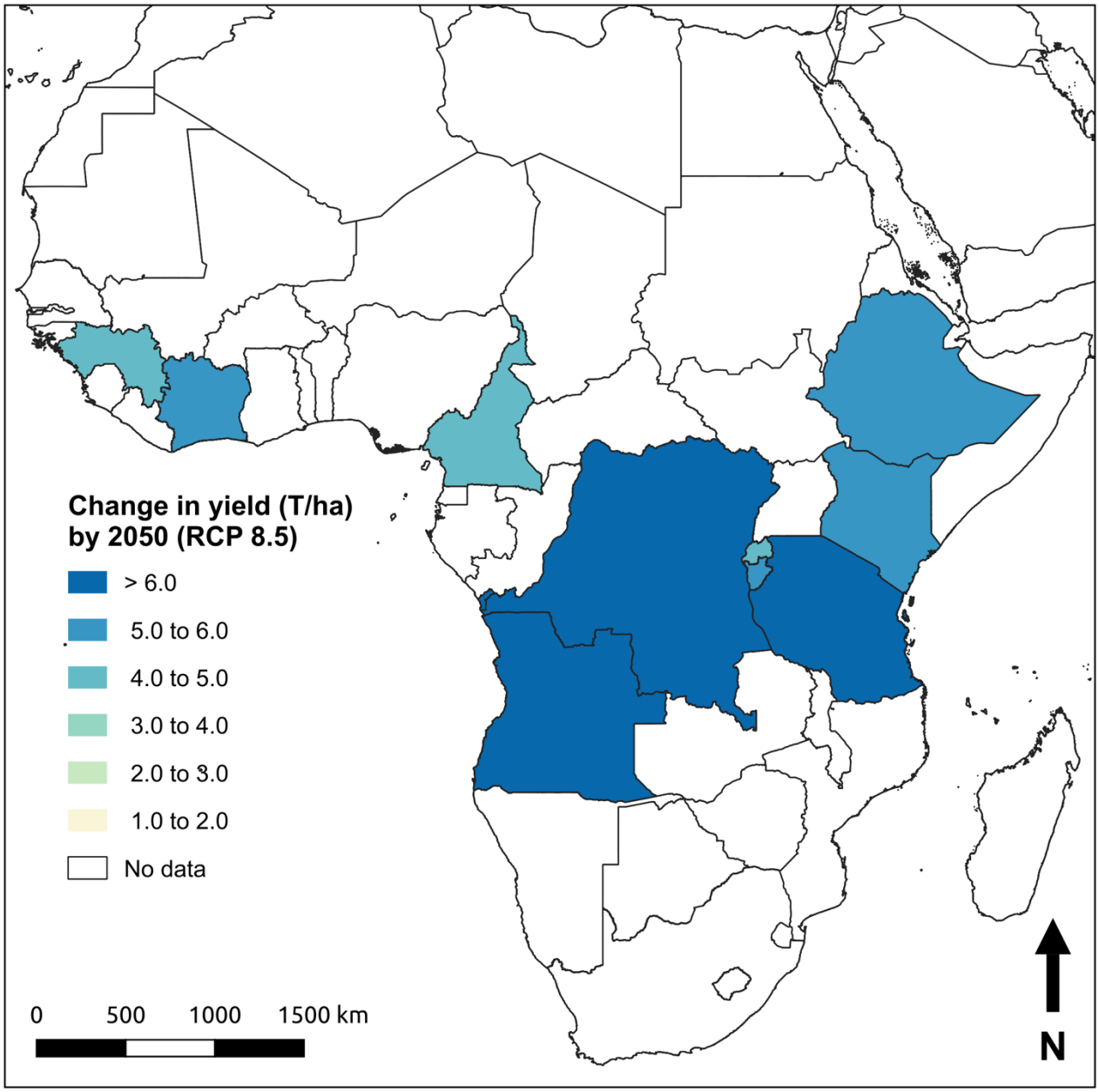

Supplementary figure S14. Map of change in forecasted yields for Africa by 2050 under the RCP 8.5 climate change scenario (relative to yields estimated using long-term climate averages between 1970-2000).

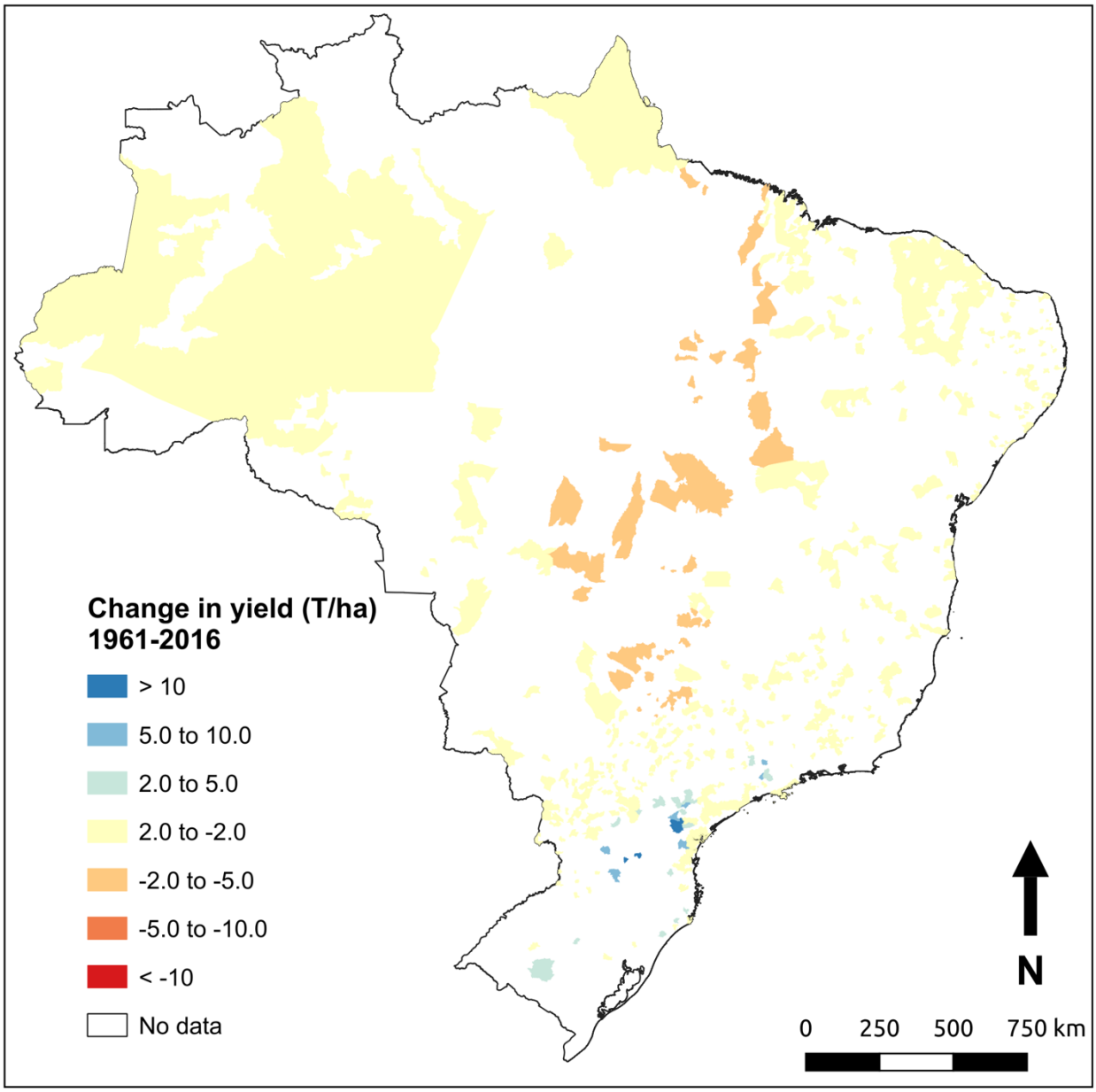

Supplementary figure S15. Map of change in yield for Brazil from 1961-2016 estimated using the hindcast analysis.

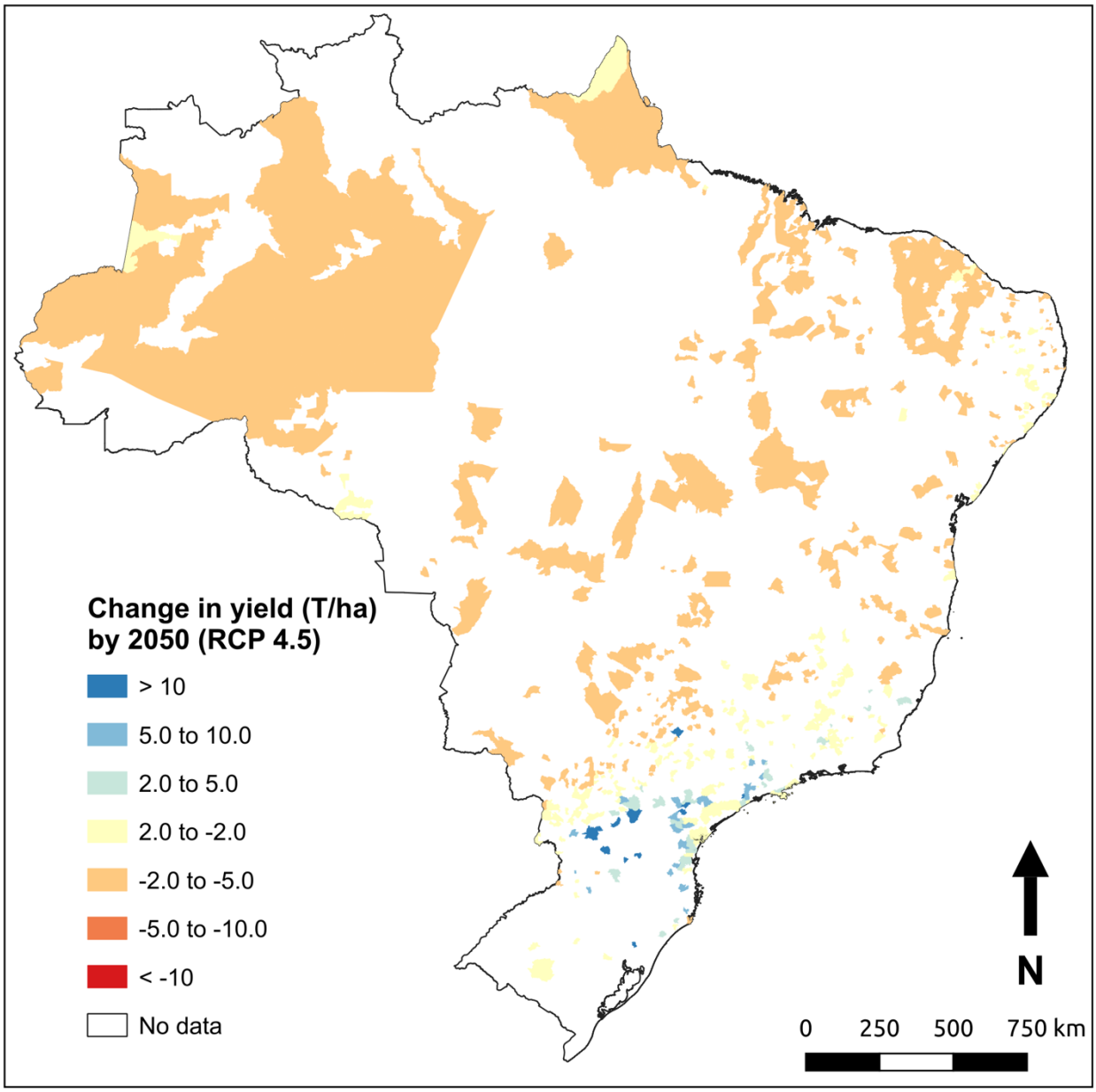

Supplementary figure S16. Map of change in forecasted yields for Brazil by 2050 under the RCP 4.5 climate change scenario (relative to yields estimated using long-term climate averages between 1970-2000).

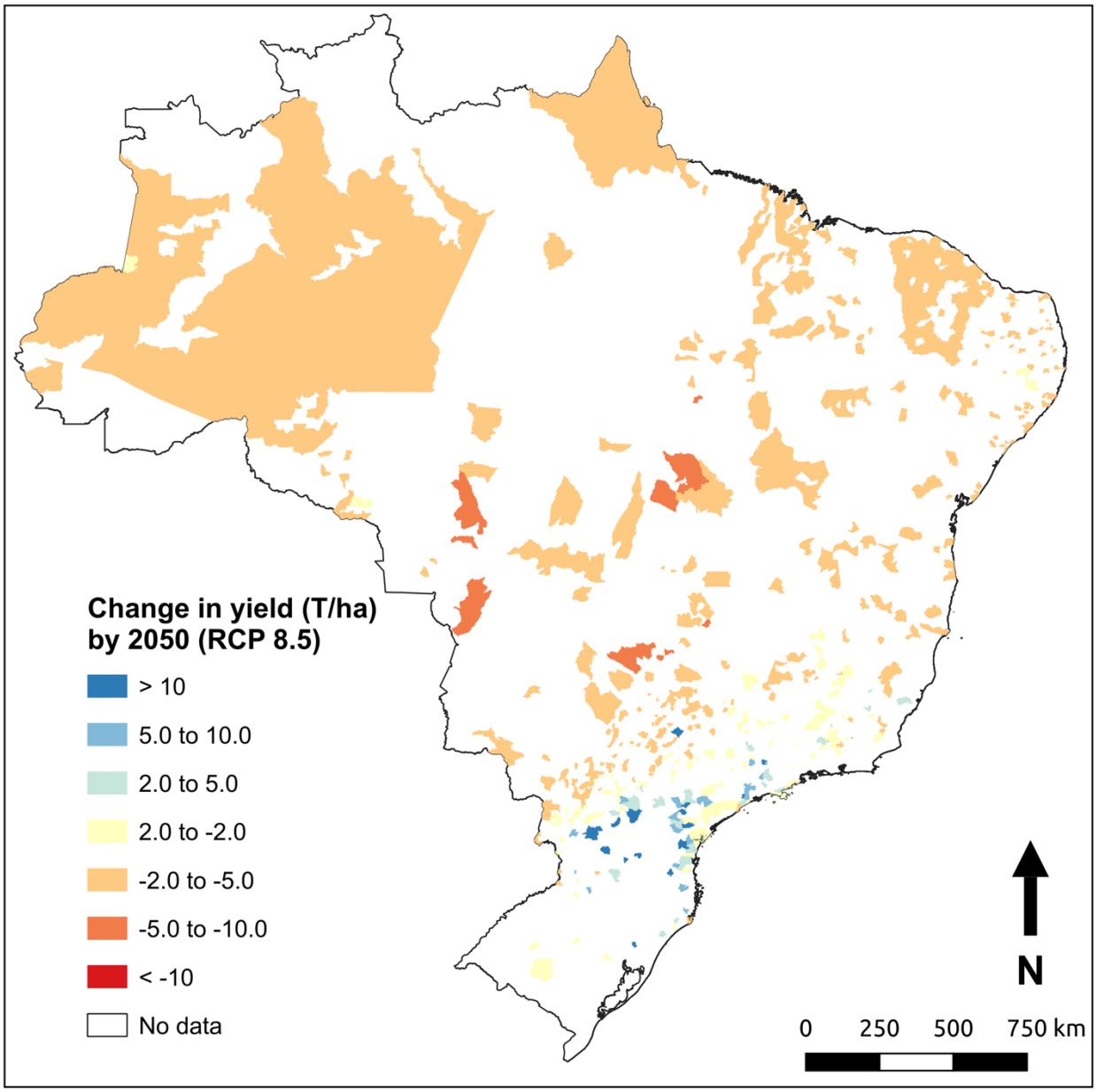

Supplementary figure S17. Map of change in forecasted yields for Brazil by 2050 under the RCP 8.5 climate change scenario (relative to yields estimated using long-term climate averages between 1970-2000).

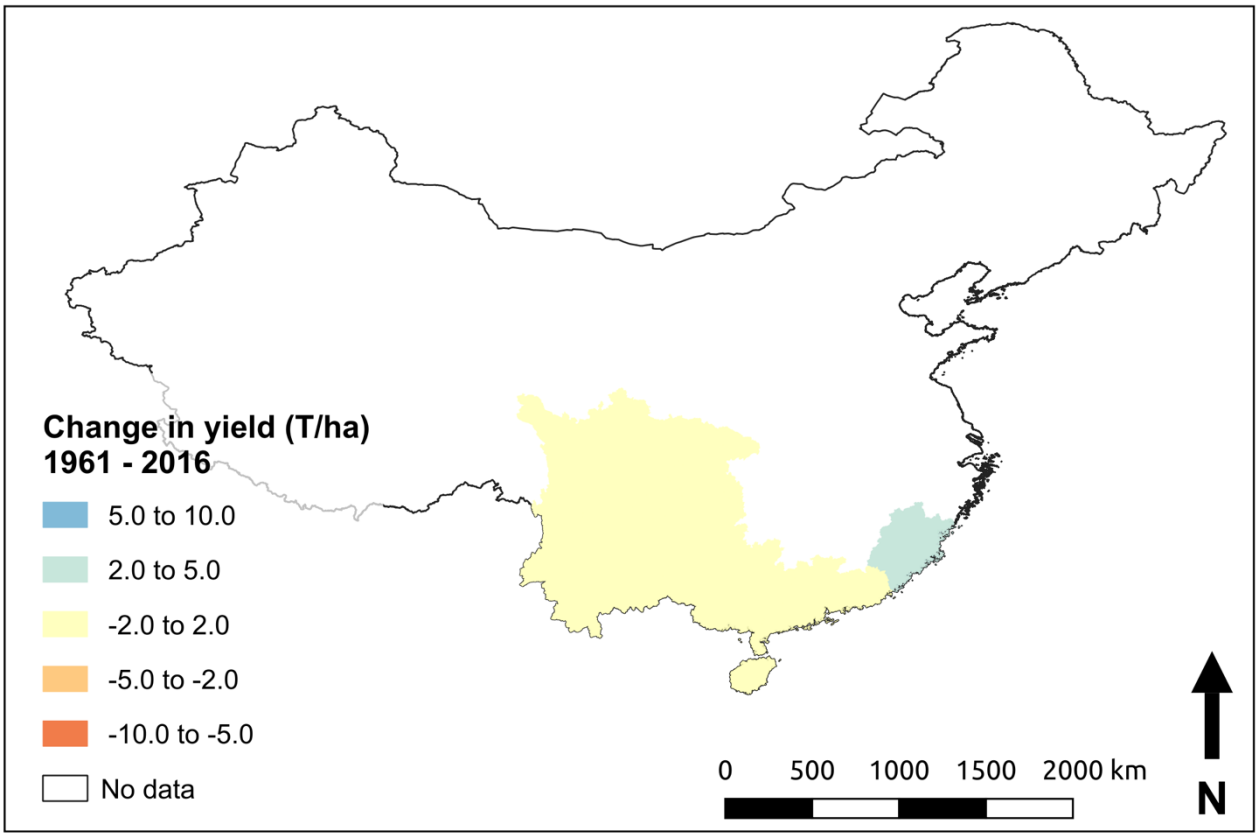

Supplementary figure S18. Map of change in yield for China from 1961-2016 estimated using the hindcast analysis.

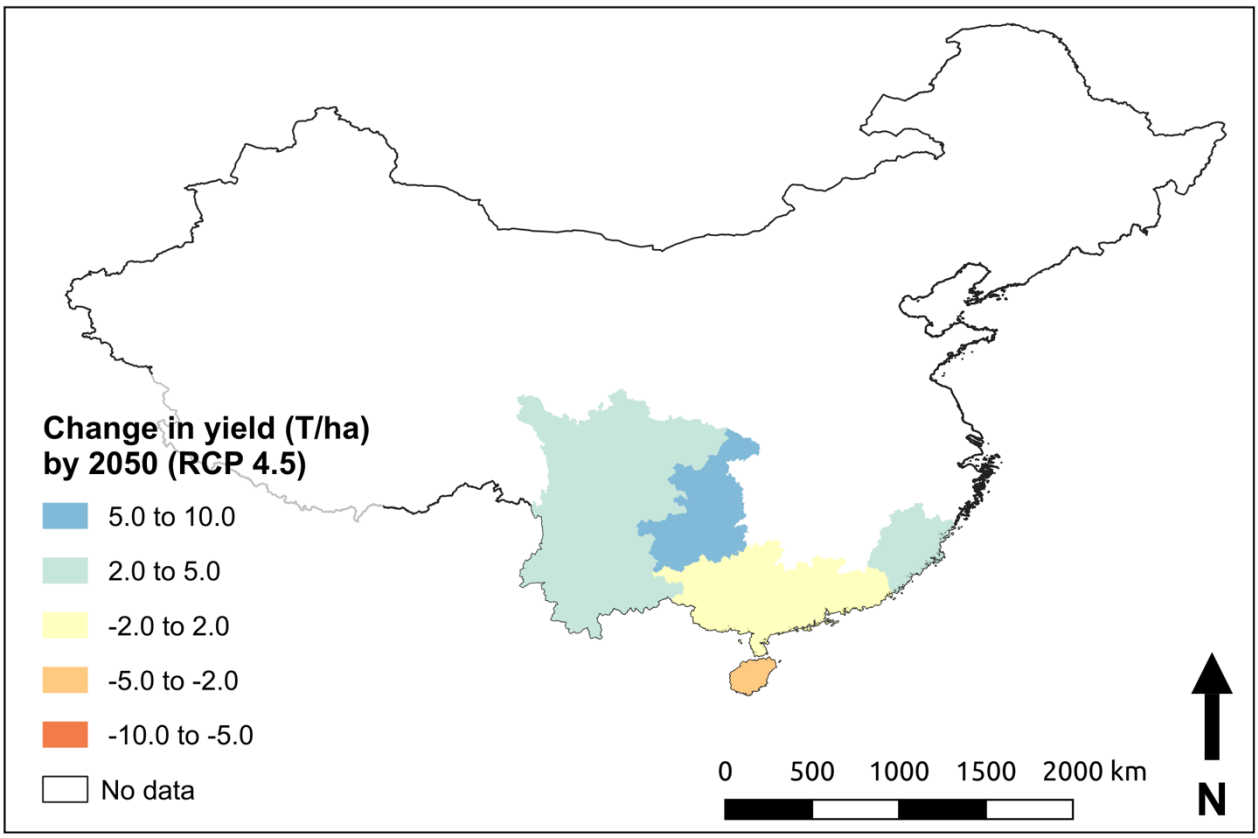

Supplementary figure S19. Map of change in forecasted yields for China by 2050 under the RCP 4.5 climate change scenario (relative to yields estimated using long-term climate averages between 1970-2000).

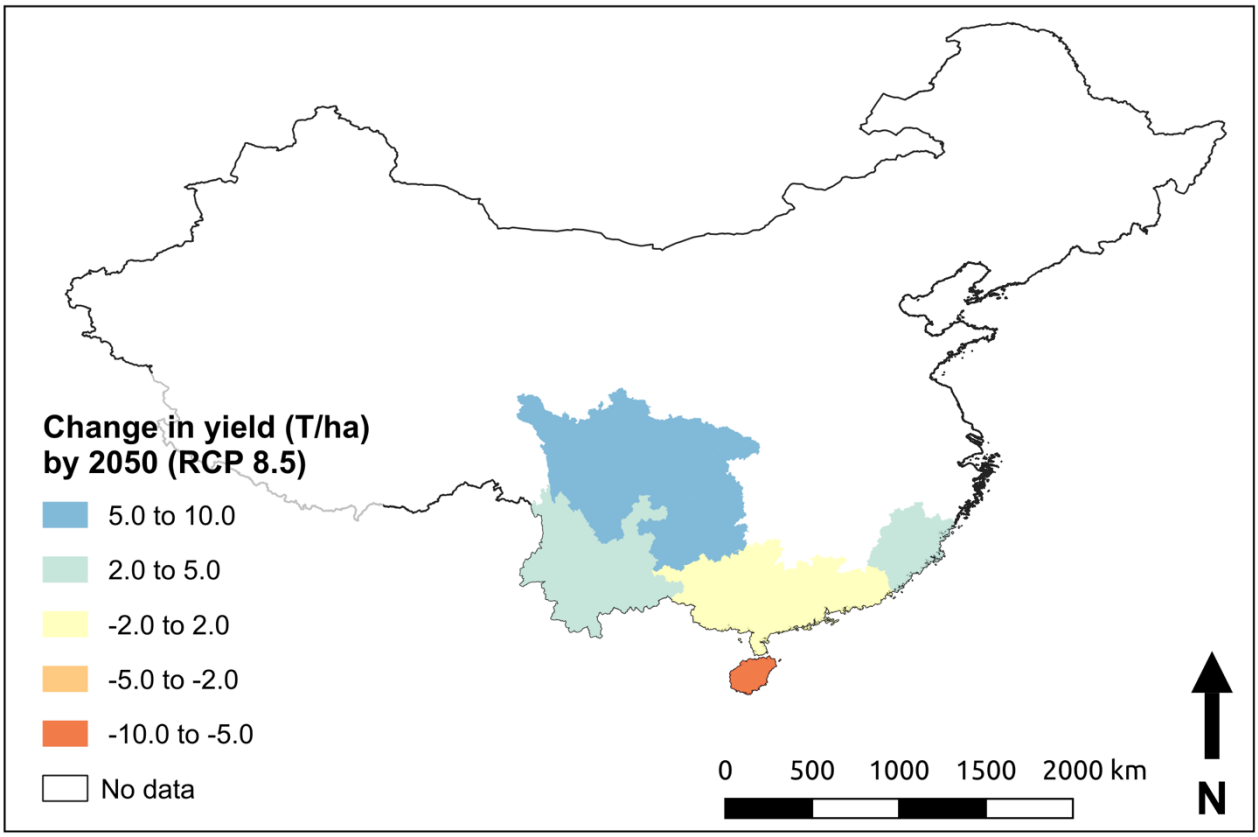

Supplementary figure S20. Map of change in forecasted yields for China by 2050 under the RCP 8.5 climate change scenario (relative to yields estimated using long-term climate averages between 1970-2000).

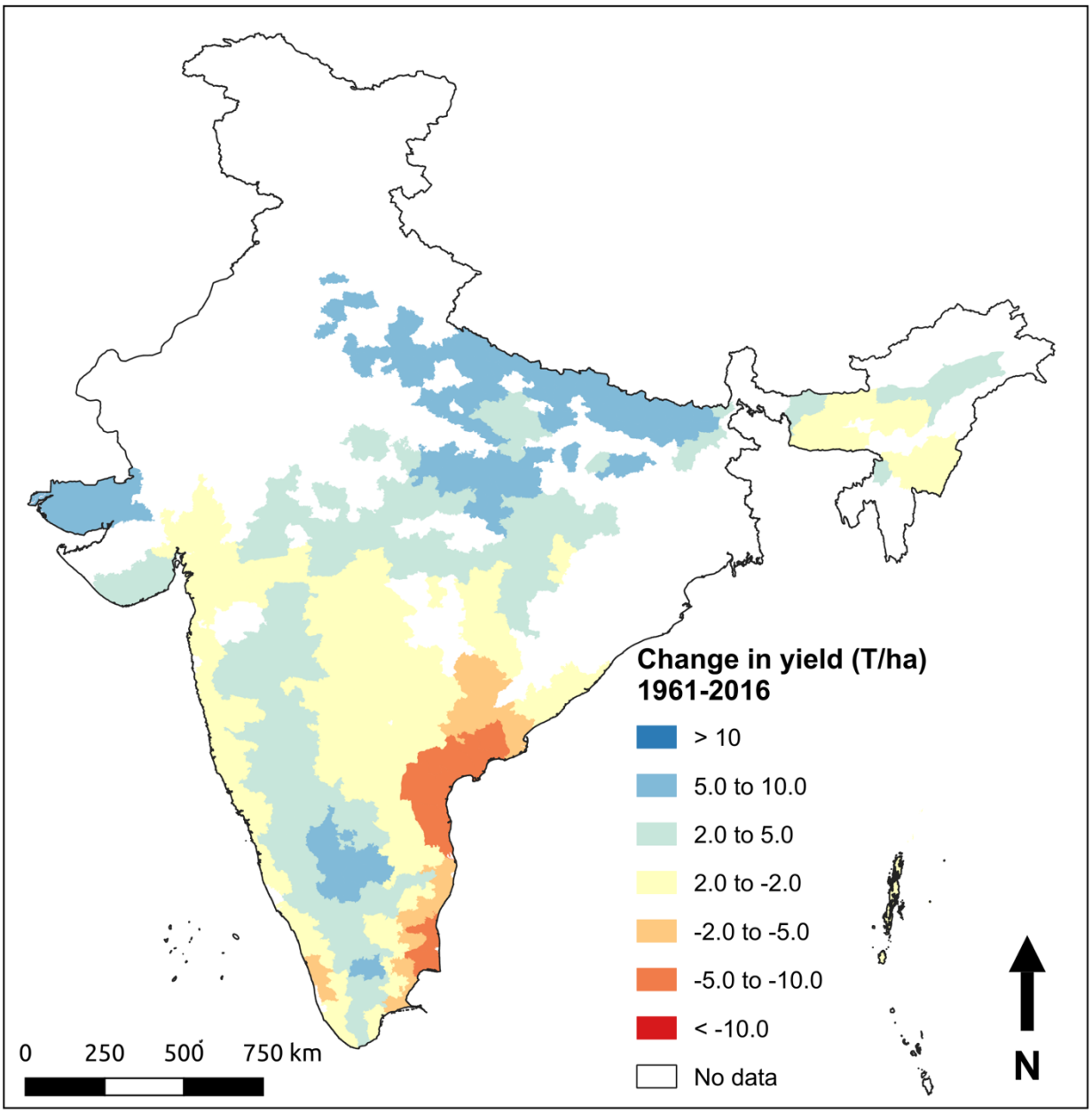

Supplementary figure S21. Map of change in yield for India from 1961-2016 estimated using the hindcast analysis.

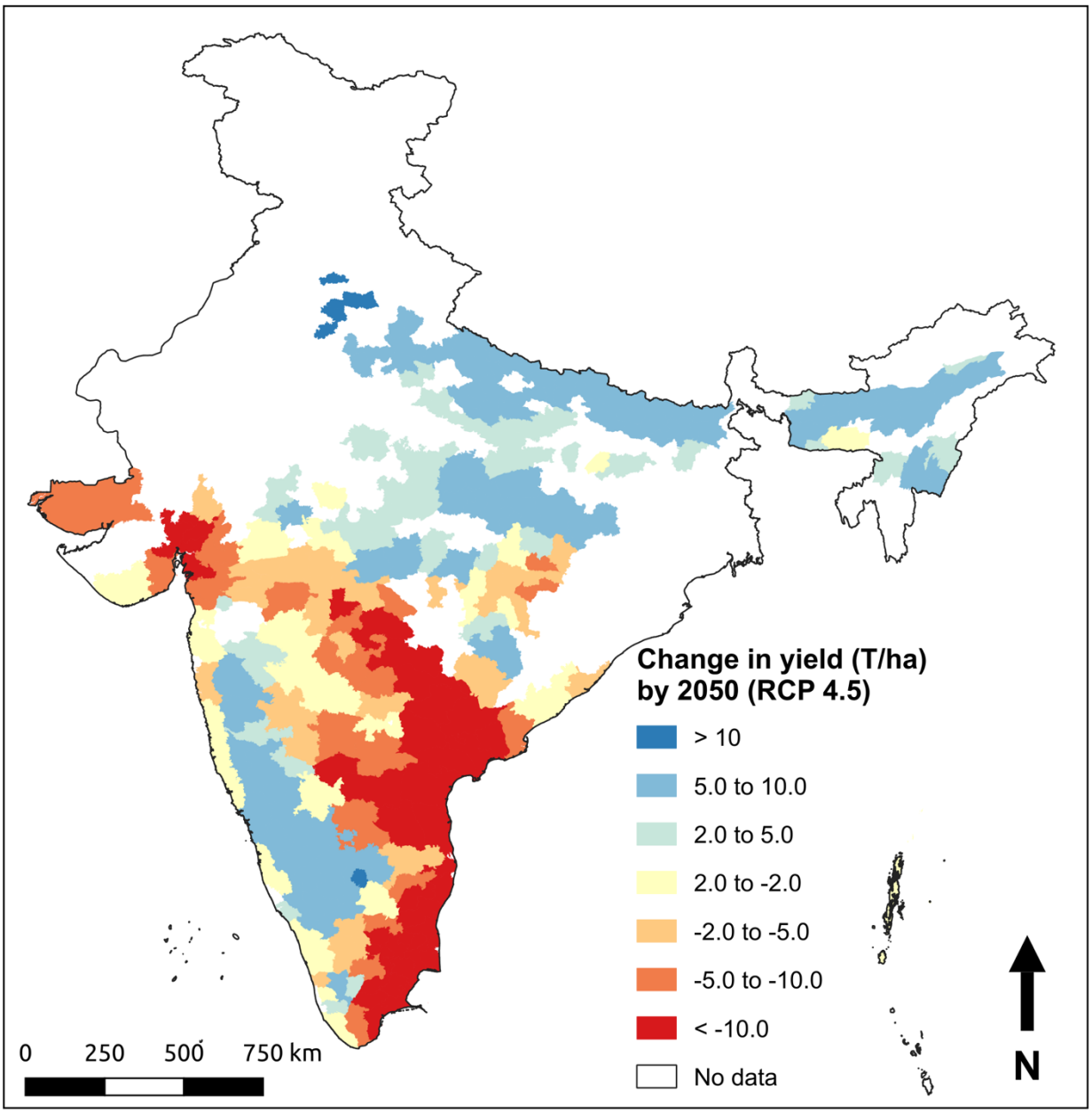

Supplementary figure S22. Map of change in forecasted yields for India by 2050 under the RCP 4.5 climate change scenario (relative to yields estimated using long-term climate averages between 1970-2000).

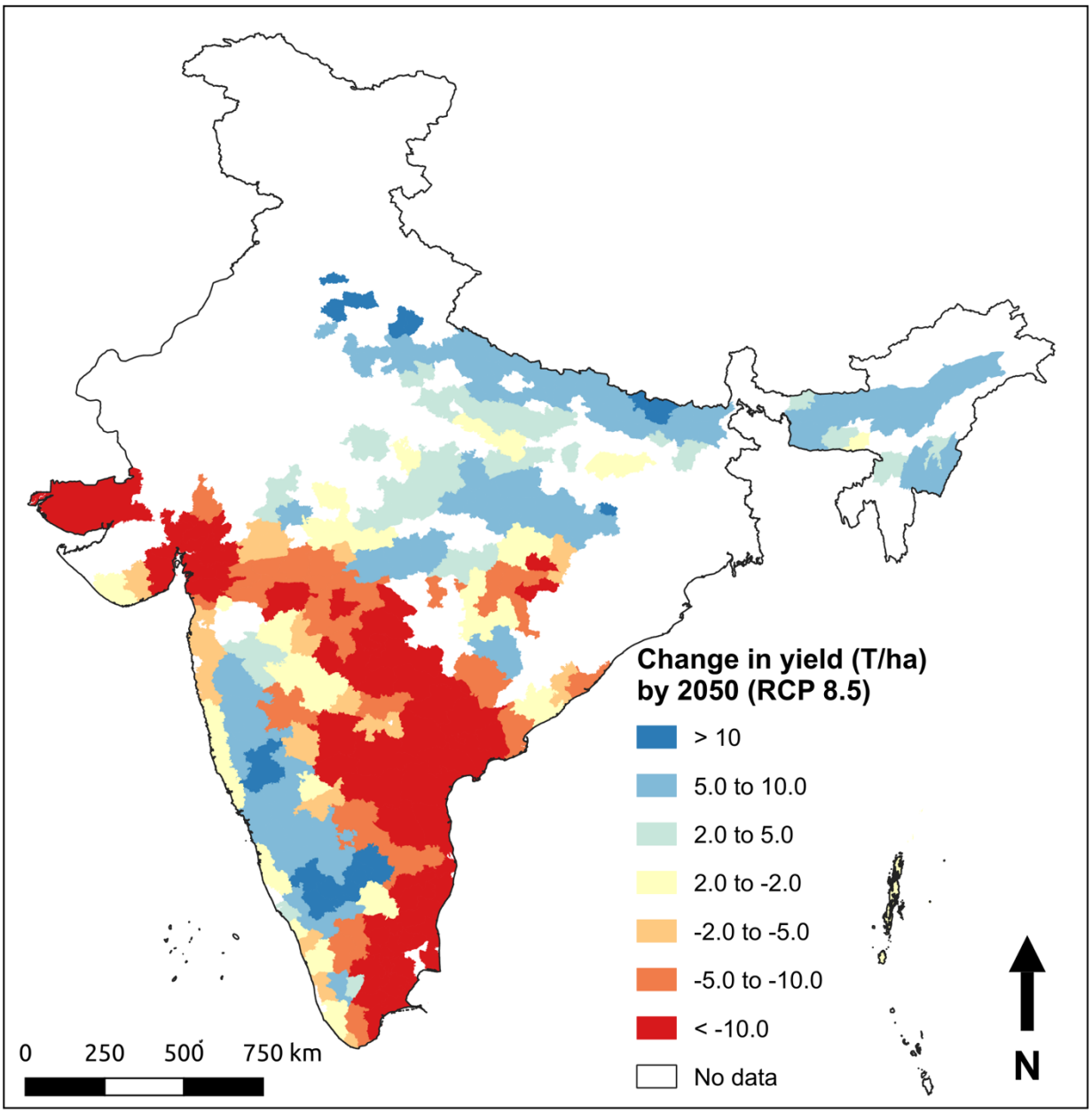

Supplementary figure S23. Map of change in forecasted yields for India by 2050 under the RCP 8.5 climate change scenario (relative to yields estimated using long-term climate averages between 1970-2000).

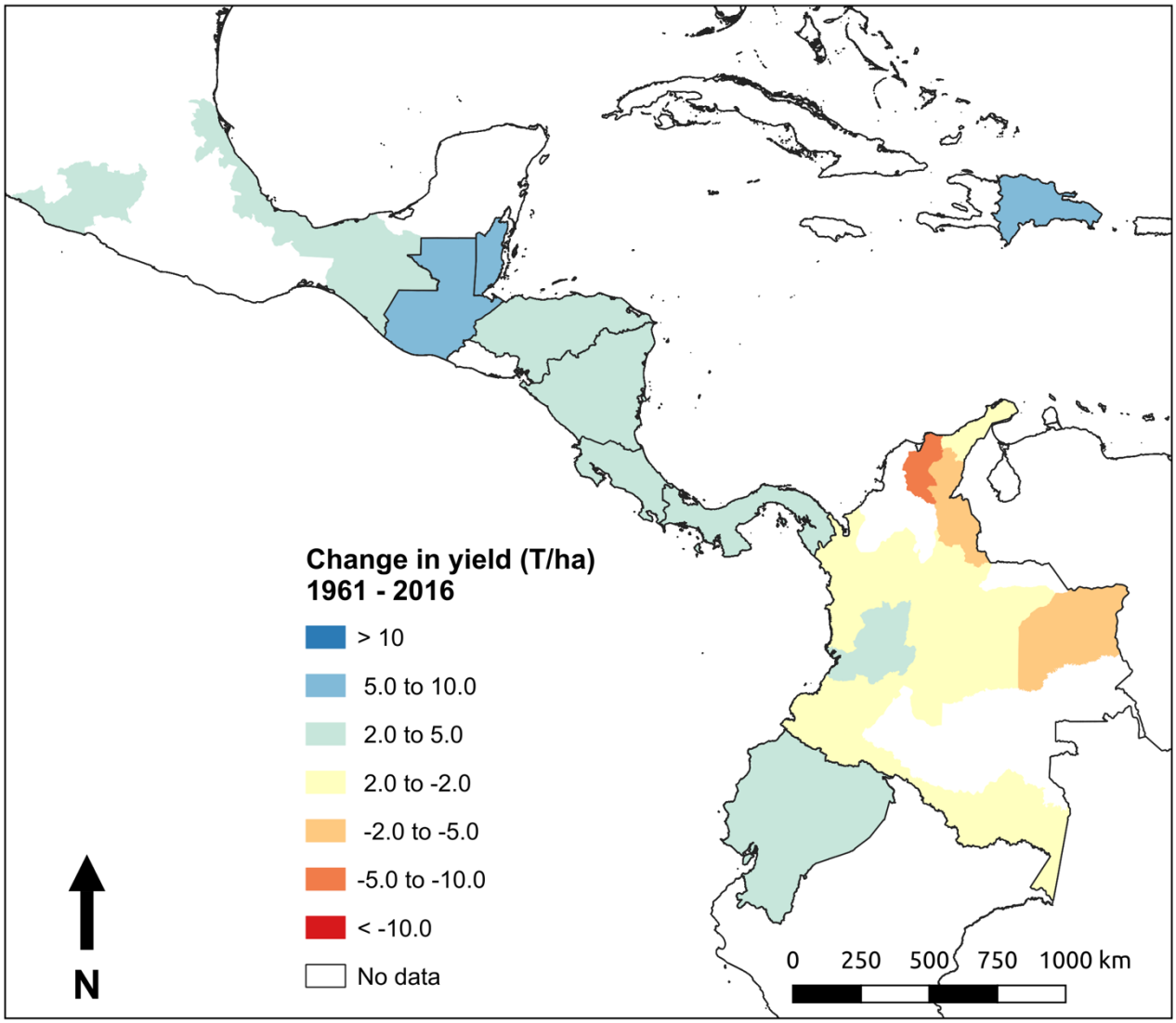

Supplementary figure S24. Map of change in yield for Latin America and the Caribbean (LAC) from 1961-2016 estimated using the hindcast analysis.

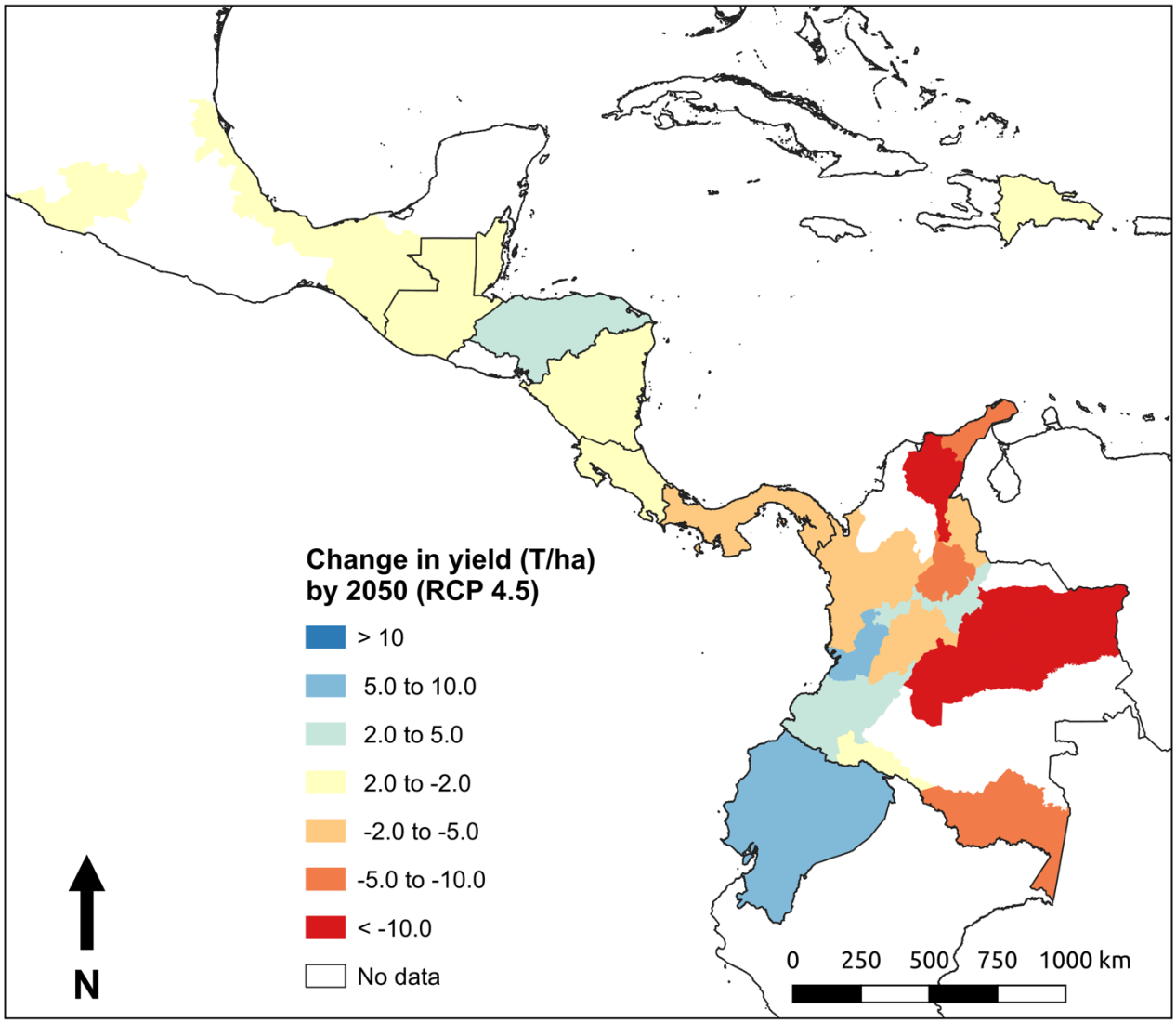

Supplementary figure S25. Map of change in forecasted yields for Latin America and the Caribbean (LAC) by 2050 under the RCP 4.5 climate change scenario (relative to yields estimated using long-term climate averages between 1970-2000).

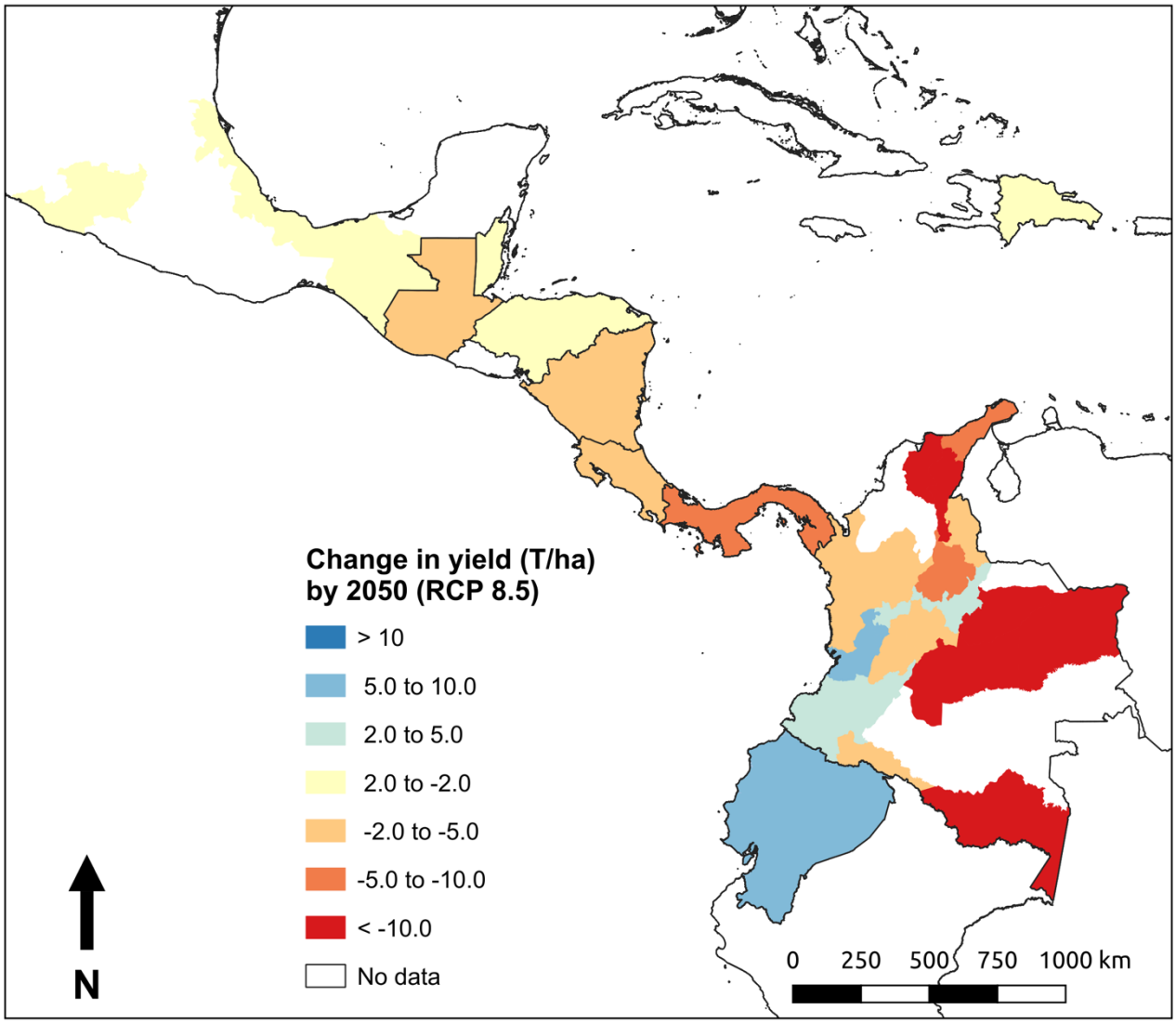

Supplementary figure S26. Map of change in forecasted yields for Latin America and the Caribbean (LAC) by 2050 under the RCP 8.5 climate change scenario (relative to yields estimated using long-term climate averages between 1970-2000).

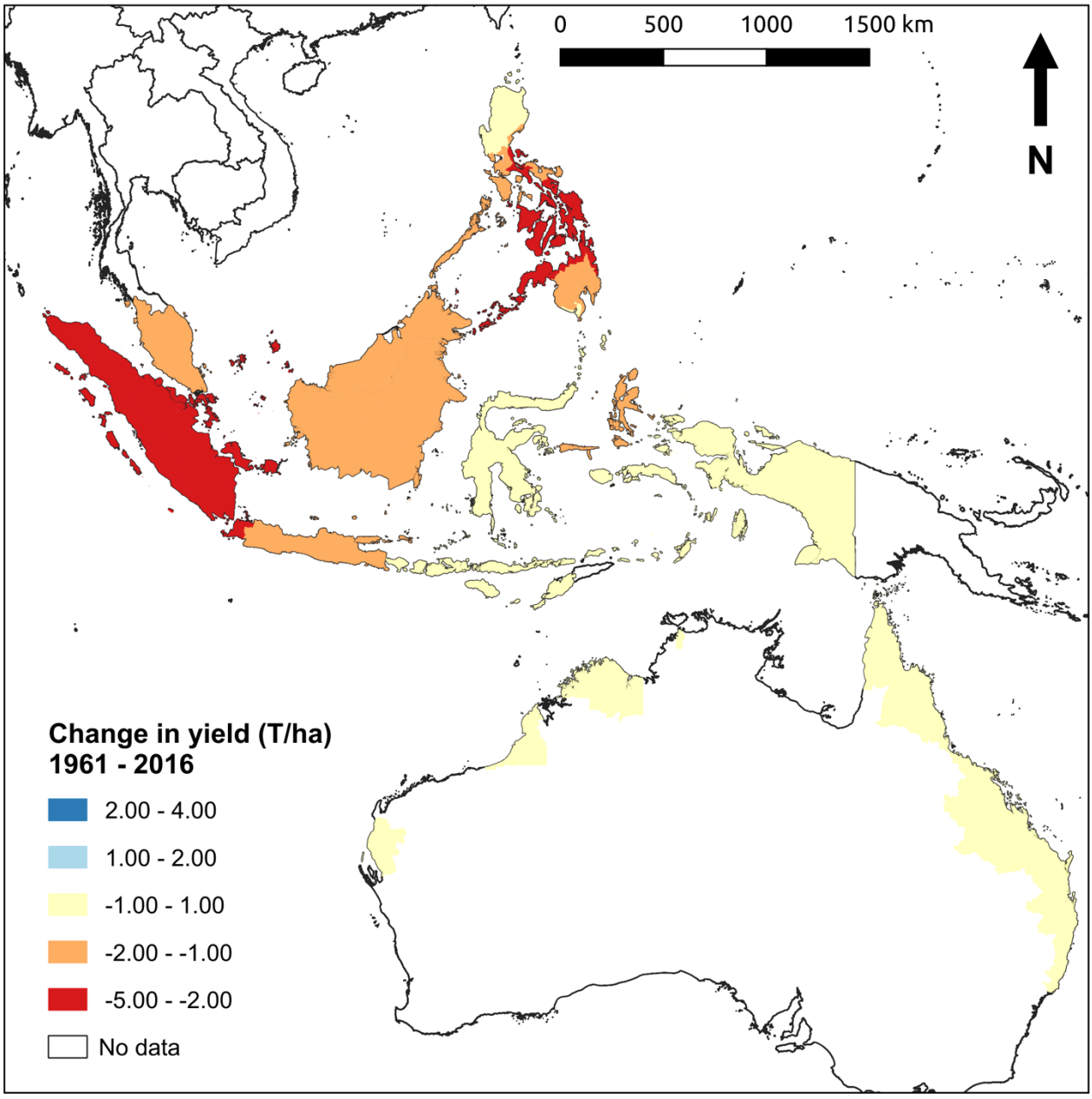

Supplementary figure S27. Map of change in yield for South-East Asia and Australia (SEAA) from 1961-2016 estimated using the hindcast analysis.

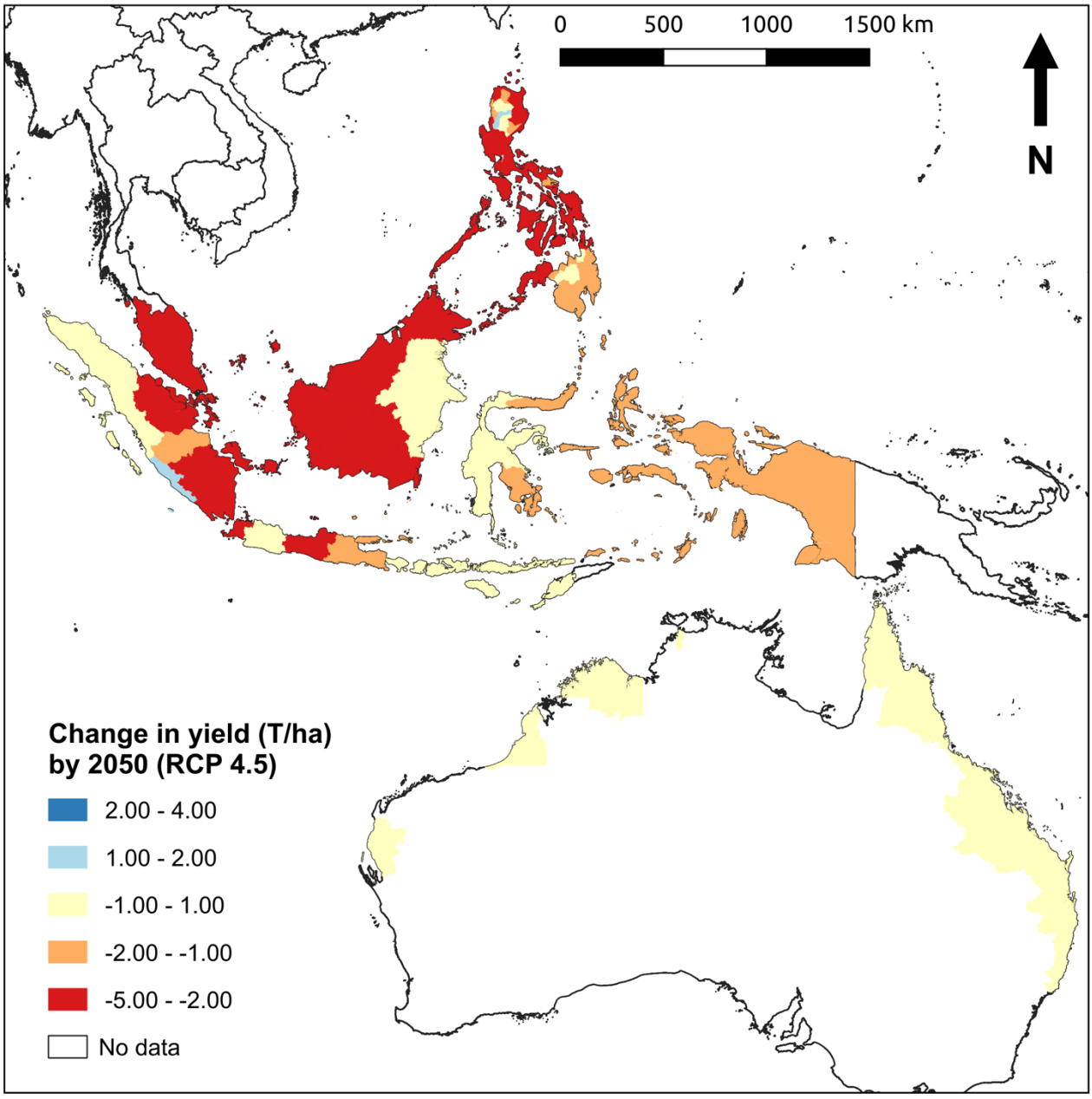

Supplementary figure S28. Map of change in forecasted yields for South-East Asia and Australia (SEAA) by 2050 under the RCP 4.5 climate change scenario (relative to yields estimated using long-term climate averages between 1970-2000).

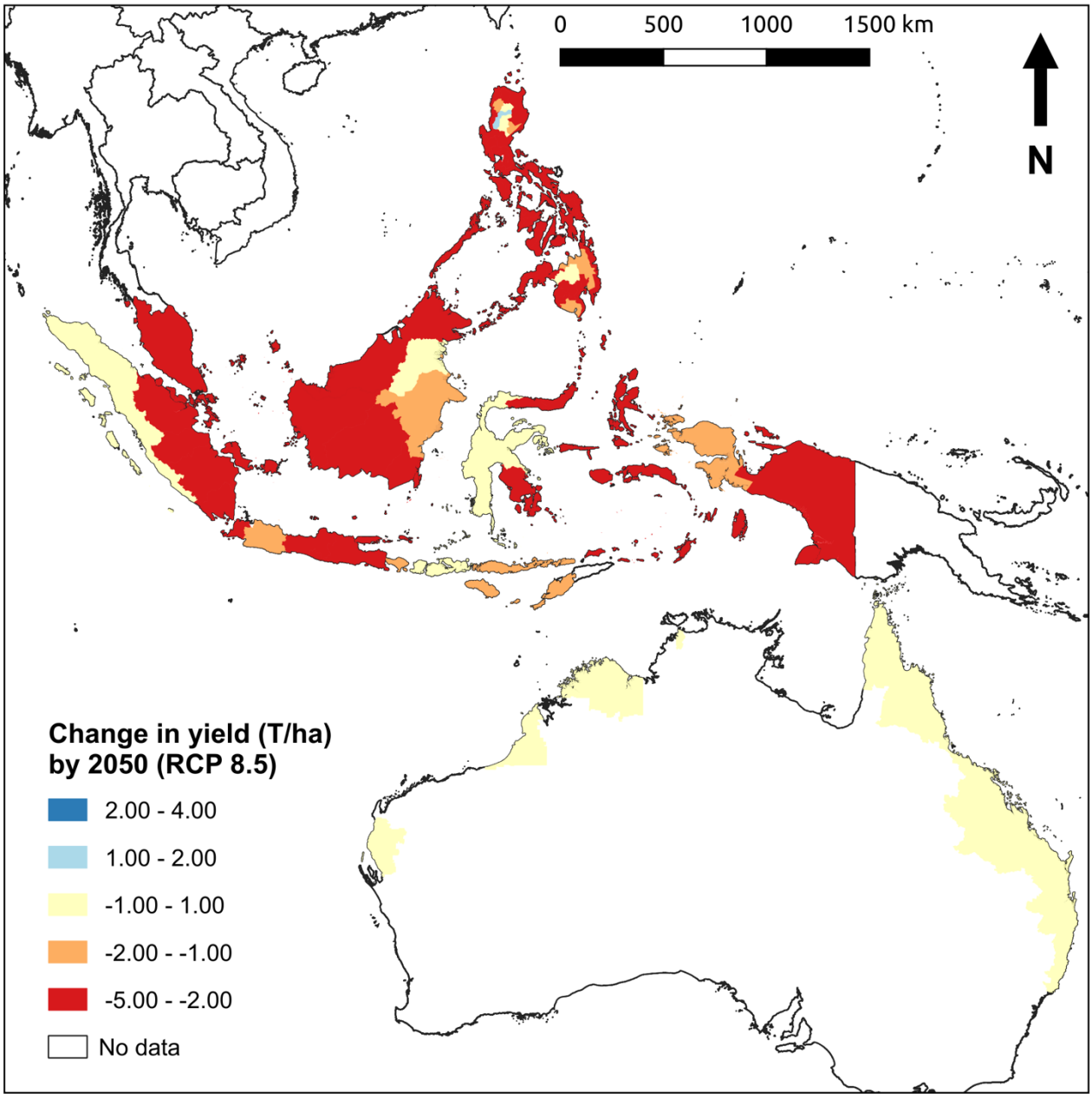

Supplementary figure S29. Map of change in forecasted yields for South-East Asia and Australia (SEAA) by 2050 under the RCP 8.5 climate change scenario (relative to yields estimated using long-term climate averages between 1970-2000).

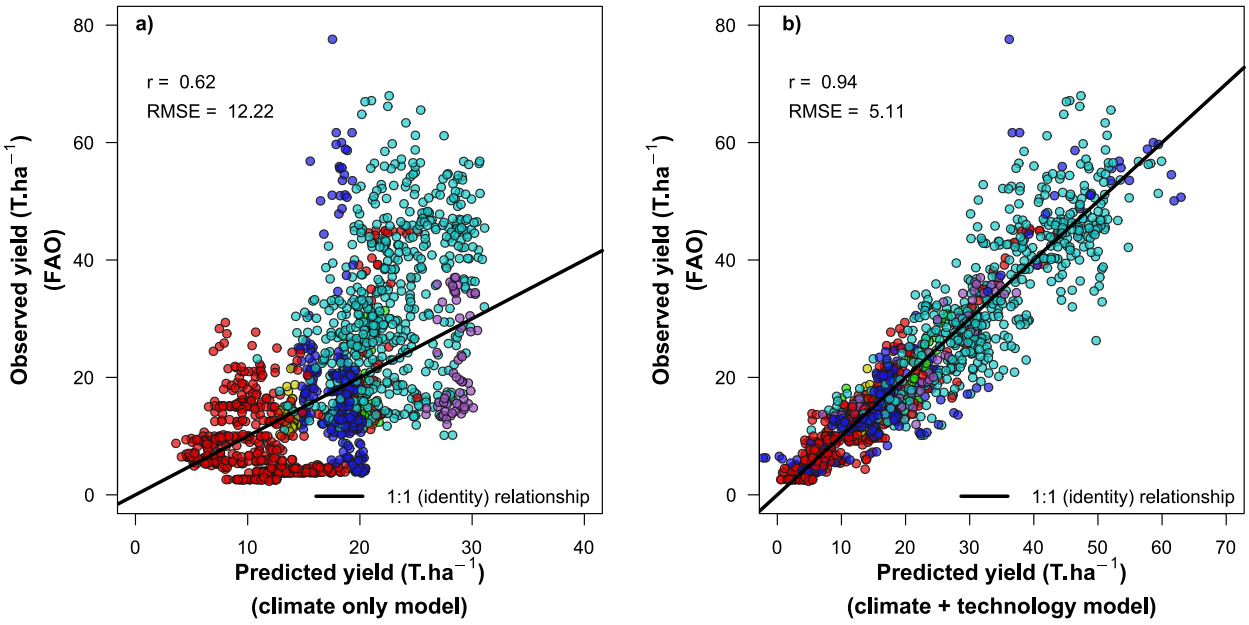

Supplementary figure S30. Fit of observed yields from FAOSTAT to yields predicted from model where only climate (temperature and precipitation) determines yield (a) and when climate and 'technology' determine yield (b). The different coloured points represent observations from the six regions in the analysis.

Appendix I – Discussion on beta model fitting procedure, visualisation and sources of variation.

To adequately model the climate sensitivity of banana productivity (yields) we require a model that is physiologically meaningful, i.e. one where along the temperature and precipitation axes contains a minimum value below which productivity will be zero, a maximum value above which productivity will be zero and an optimum value where productivity is maximised. For obvious reasons the optimum value will fall somewhere between the minimum and maximum. However, we need to also ensure that the optimum value is flexible, i.e. there should be no requirement that it falls at the mid-point between the minimum and maximum values, nor should it be biased towards either the minimum or maximum. The beta function employed in these analyses meets these criteria. Since we are modelling yield as a function of both temperature and precipitation, a beta function fit along both these axes will result in a three-dimensional surface as illustrated in figure A1 below.

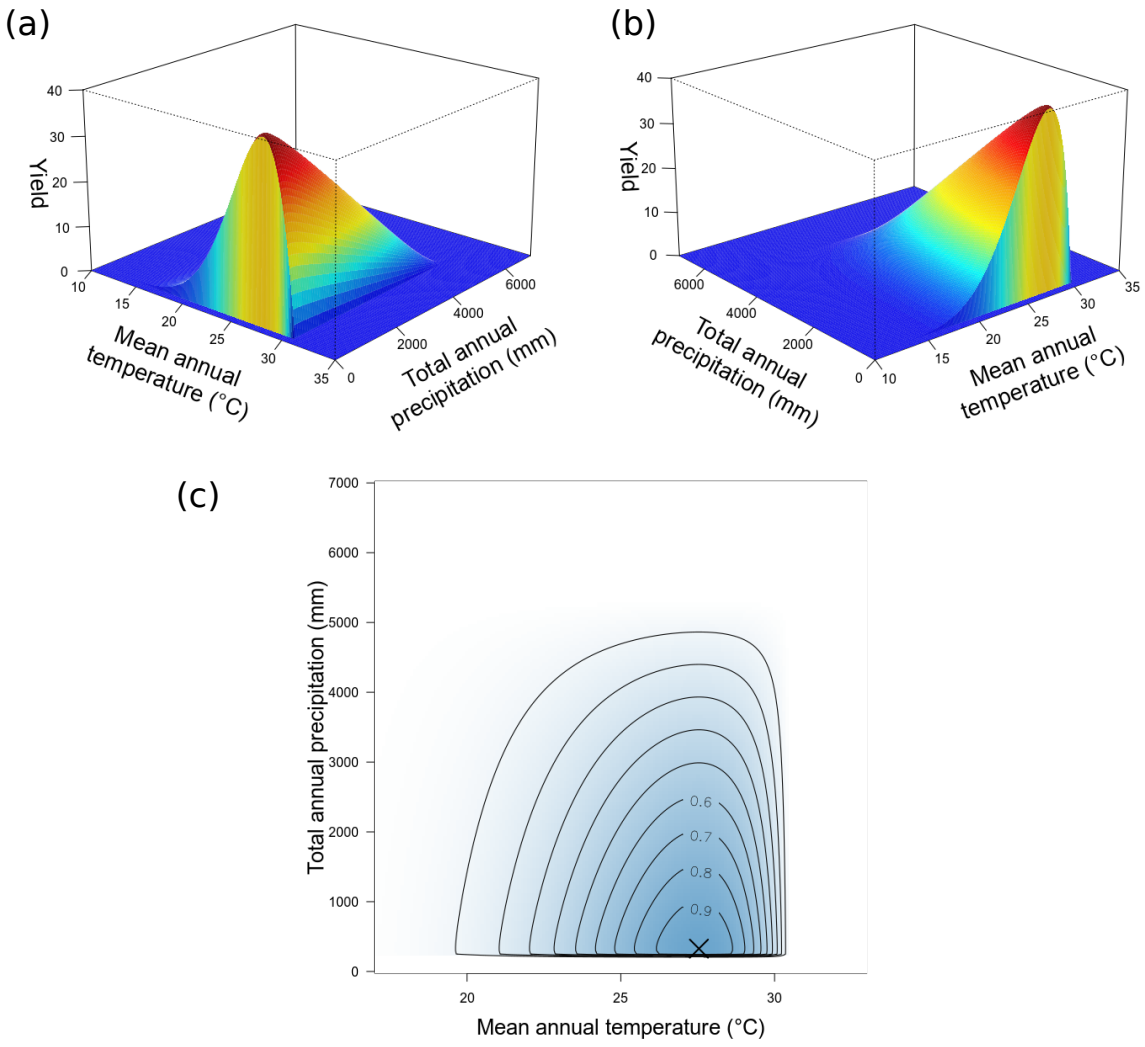

Figure A1. Three dimensional representation of the beta model fitted to yield data from India. Panels (a) and (b) are the same surface of yield as a function of both mean annual temperature and total annual rainfall and viewed from two different angles for clarity. The model is also visualised as a contour plot (c) where 'X' indicates the temperature and precipitation combination where yield is maximised. Values on the contour lines are proportional to the maximum, i.e. values of 0.9, 0.8, 0.7, etc. represent yields of 90%, 80%, 70% and so on, relative to that at the maximum.

As outlined in the Methods section, the model fitting procedure needs to estimate seven parameters for each climate-yield dataset (i.e. regional data subsets). The brute-force method we employed searched through 10 million parameter combinations for this estimation (for each data subset), by looking for the parameter combinations which result in the lowest residual sums of squares. To be more confident of the results, we then used the brute-force estimates as starting values in a non-linear curve fitting procedure, which we bootstrapped using 100 iterations to arrive at the final set of parameters. The method employed results in robust estimates of the beta function, i.e. it varies very little if the procedure is repeated on the same dataset. Hence, our model if fit objectively to the data, and our inferences are an objective empirically-grounded interpretation of the best fit models. The model fitting process results in parameter estimates that are utilised to create the three-dimensional surface (as illustrated in figure 1, above). This surface represents the 'average' expected yield for combinations of mean annual temperature and total annual precipitation for the region. Observed yield values can show scatter around this surface for the same temperature-precipitation combinations as a result of unaccounted for sources of variation at the model fitting stage. We address some of these sources of variation later in this section.

The fitted curves (panels (a) and (b) in supplementary figures 1-7) represents cross sections of the three-dimensional surface that is produced using the estimates parameters for each regional data subset. A schematic illustration of these cross sections are presented in figure A2, below. Hence, panel (a) (in supplementary figures 1-7) is a cross section along the temperature axis when precipitation is held at its optimum, while panel (b) of the supplementary figures (1-7) is a cross section along the precipitation axis when temperature is held at its optimum. Hence, the fitted lines in supplementary figures 1-7 represent the change in average yield with change in one climate variable when the other is held at its optimum.

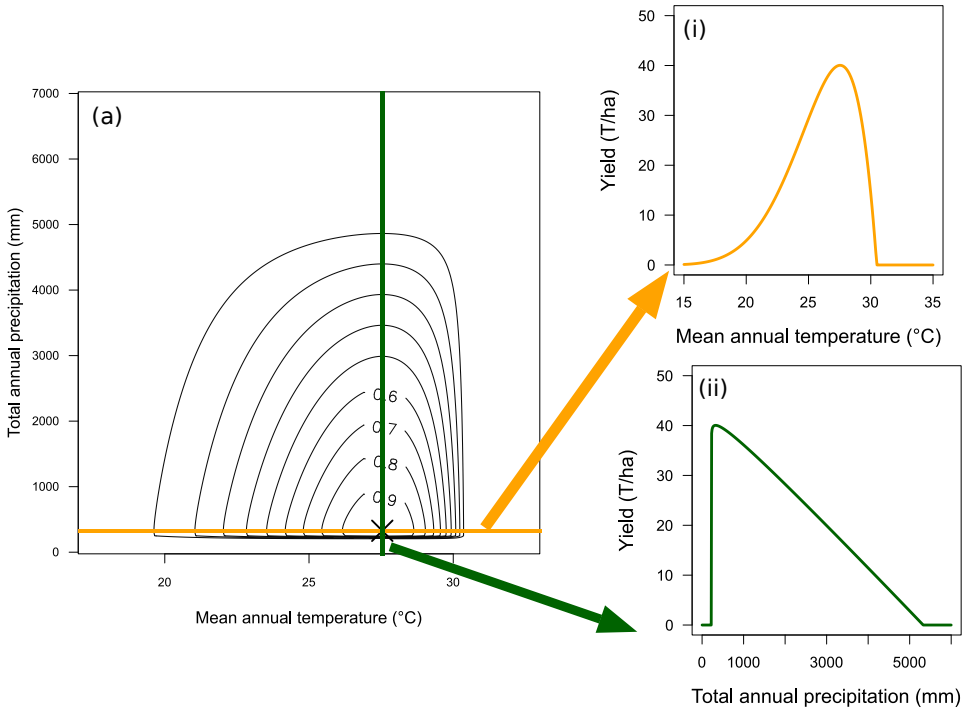

Figure A2. Panel (a) is a contour plot that represents the beta function fitted to yield data from India. The orange line represents the cross section of the three-dimensional model surface, where precipitation is held constant (at its optimum) and temperature is allowed to vary. This results in panel (i) that is also presented in supplementary figure 4a. The green line is a cross section of the three-dimensional surface when temperature is held at its optimum and precipitation is allowed to vary. This results in panel (ii) which is presented in supplementary figure 4b.

The variation around the curves presented in supplementary figures 1-7 comes from multiple sources. First, supplementary figures 1-7 are two-dimensional representations of data and model fits that are spread across three dimensions. Hence, panels (a) and (b) are flattened views of the data, through which the best fit line along only two dimensions is visualised. If we consider one of these – e.g. the India dataset plotted along the temperature axis (supplementary figure 4a – relationship of yield with temperature when precipitation is held at its optimum) and also plot additional curves representing the yield relationship to temperature at precipitation values greater than the optimum (327 mm) e.g. 1000 mm, 2000 mm, 3000 mm and 4000 mm, we get the figure A3 below. When data are present at these combinations of temperature and precipitation, on average they will occupy space on the graph represented by these new curves. Hence, all data taken together will appear as scatter around the curve representing optimum precipitation.

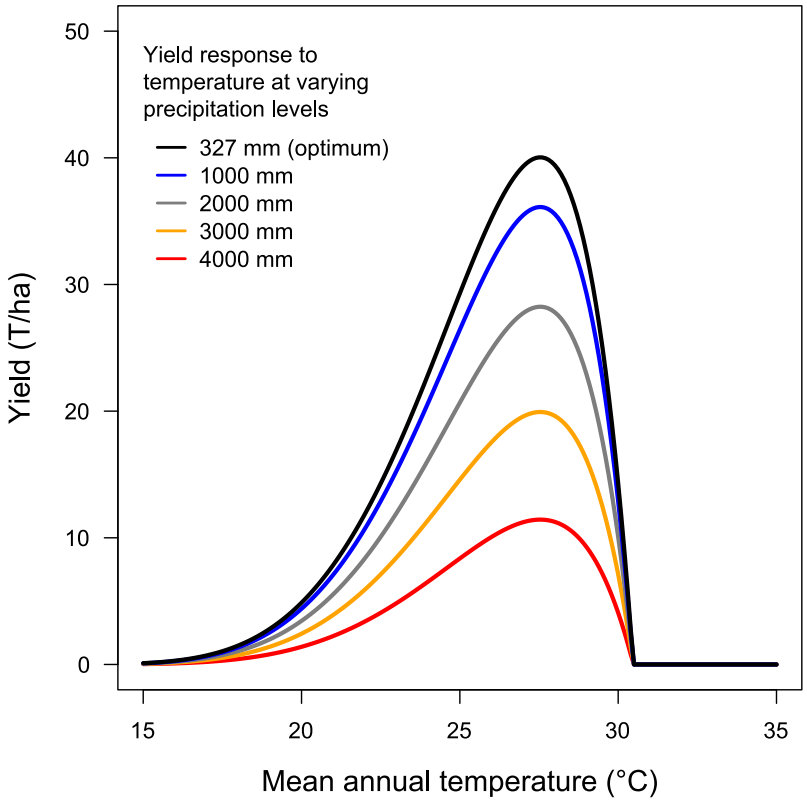

Figure A3. Model fit for India of average yield as a function of temperature, when precipitation is held at at optimum (327 mm; black line), and with precipitation levels greater than the optimum, i.e. 1000 mm (blue), 2000 mm (grey), 3000 mm (orange) and 4000 mm (red). This is a two-dimensional representation of a three-dimensional surface presented in figures 1a and 1b, above. The curve presented in manuscript supplementary figures 4a is a similar representation for the curve at optimum precipitation (black line here), but with 'all' data points (i.e. for all precipitation levels) also presented. This contributes to some of the scatter around the curve in supplementary figure 5a.

The second source of scatter is from unaccounted for variation – such as from variation in use of irrigation, fertiliser inputs, etc. in planting areas which may share the same temperature and precipitation regimes. Some of this variation is assessed in our analysis of technology trends. But this occurs after the model fitting procedure. Other sources of variation (e.g. use of irrigation) are not explicitly accounted for in our analyses due to lack of usable data of consistent quality across the regions assessed. In addition, the implicit inclusion of irrigated cultivation in the production datasets could influence beta function parameter estimates for precipitation. Hence, optimum precipitation estimates should be interpreted with care.